

# MACROSCOPIC DEGENERACY AND FRAGMENTATION IN THE XY MODEL ON THE KAGOME LATTICE

ALEXEI ANDREANOV

APFM2018, ICTS BENGALURU,

DEC 5, 2018

---

*PS*  
*C* Center for Theoretical  
Physics of Complex Systems





MIKHAIL FISTUL

arxiv:1801.03842 + in progress



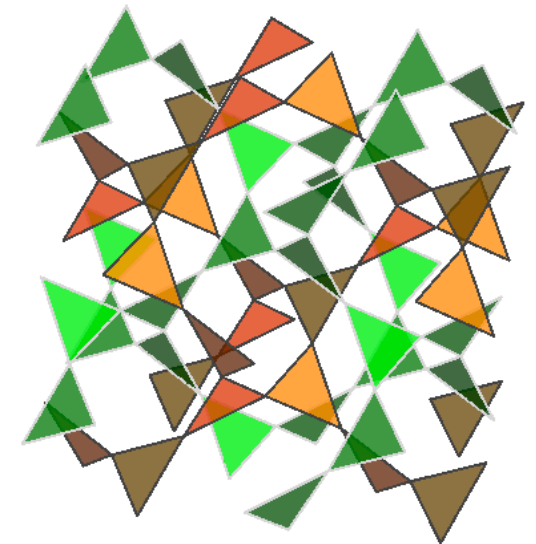
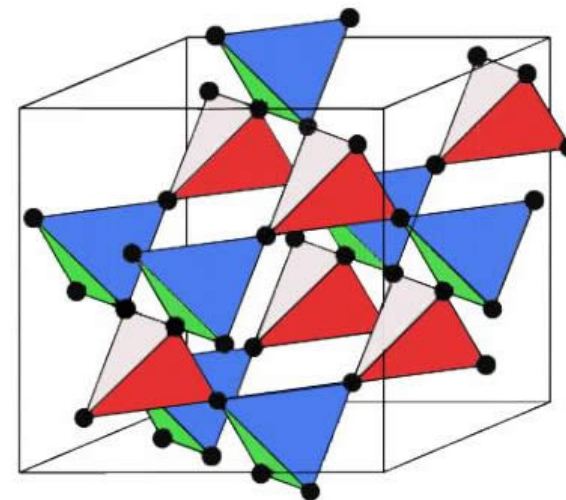
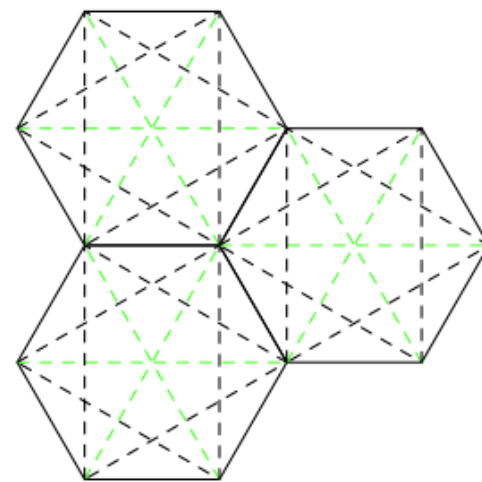
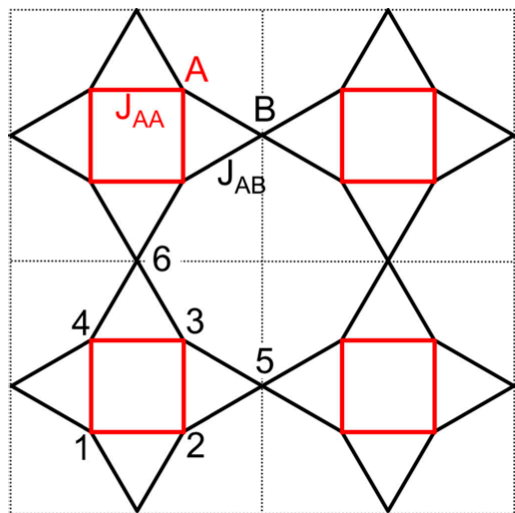
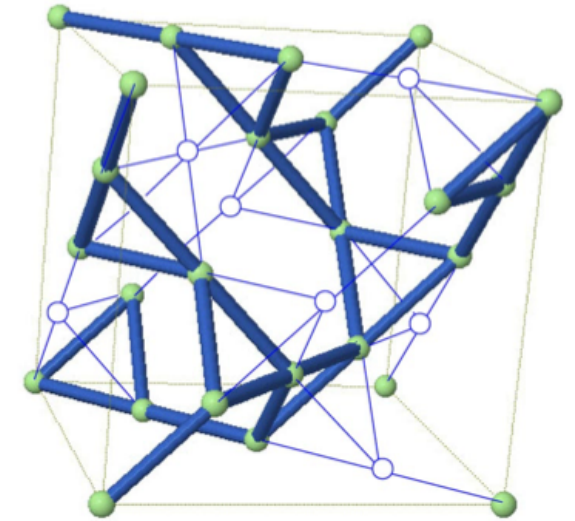
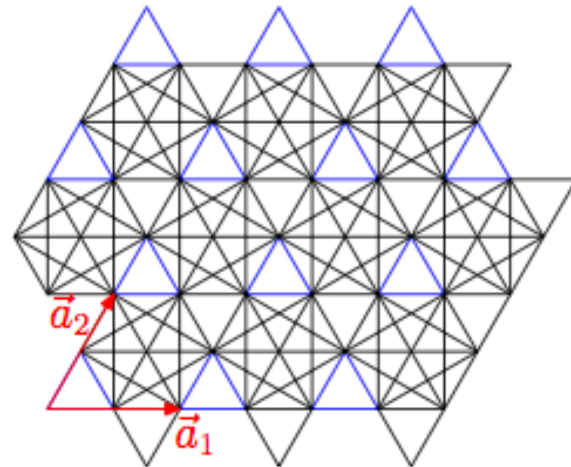
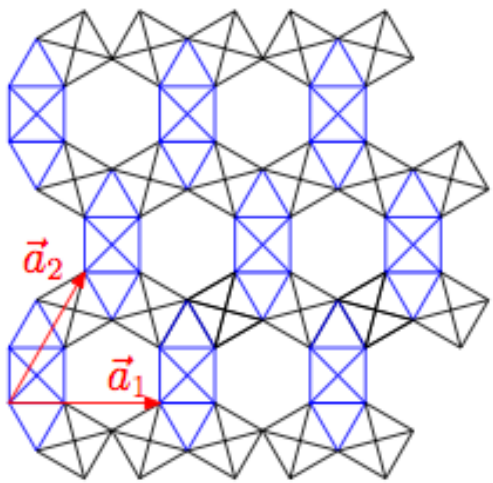
# IBS CENTER FOR PHYSICS OF COMPLEX SYSTEMS





# FRUSTRATION

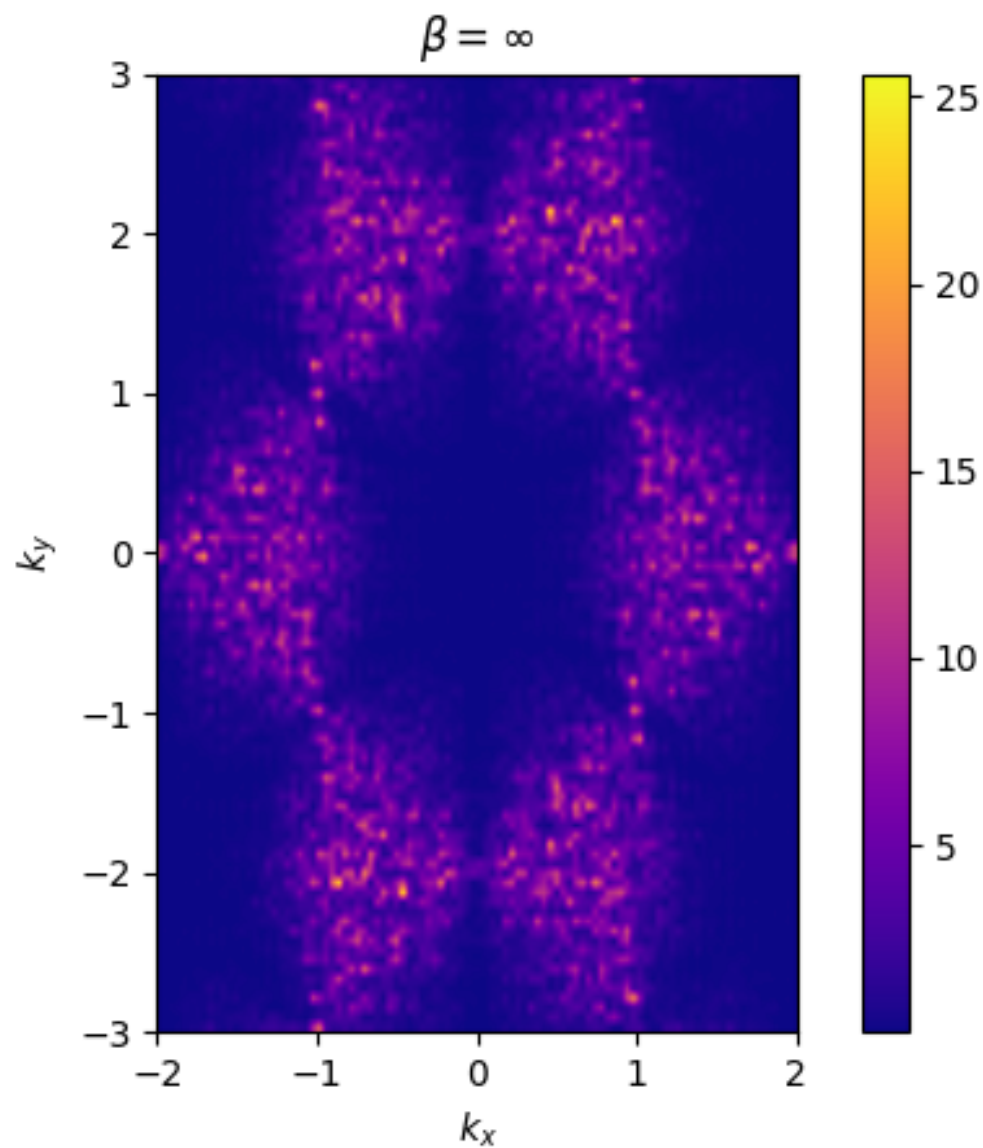
$$\mathcal{H} = - \sum_{ij} J_{ij} S_i S_j$$



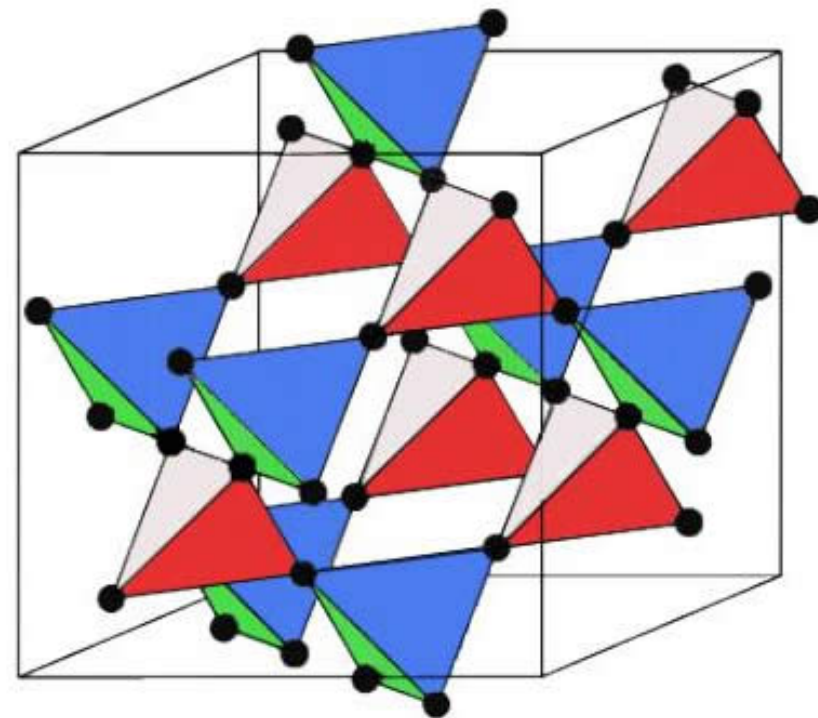
# COULOMB PHASES AND SPIN LIQUIDS

$$\mathcal{H} = - \sum_{ij} J_{ij} s_i s_j = -J \sum_{\Delta} S_{\Delta}^2 \quad S_{\Delta} = \sum_{i \in \Delta} s_i$$

Groundstates:



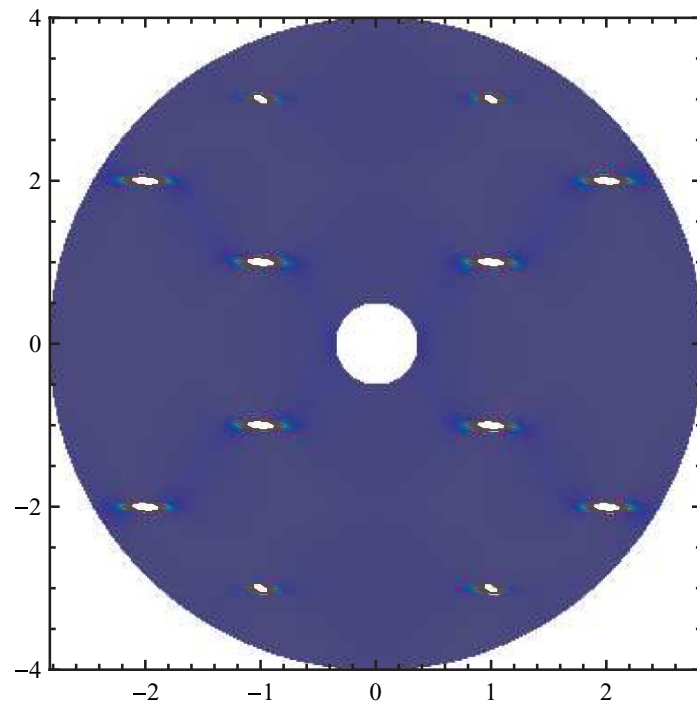
$$\forall \Delta \quad S_{\Delta} = 0$$



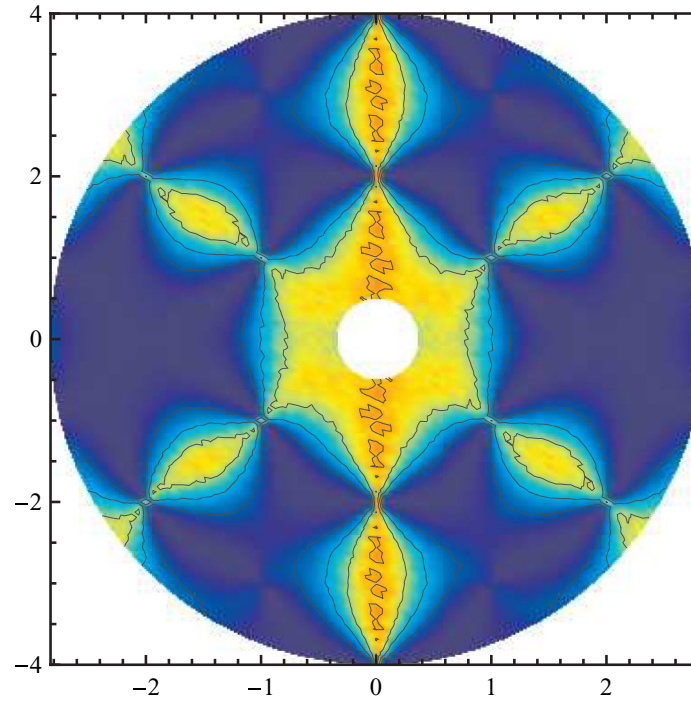
# **PART 1 – MAGNETIC FRAGMENTATION**

# MAGNETIC MOMENT FRAGMENTATION

Ordered phase



Cooperative paramagnet

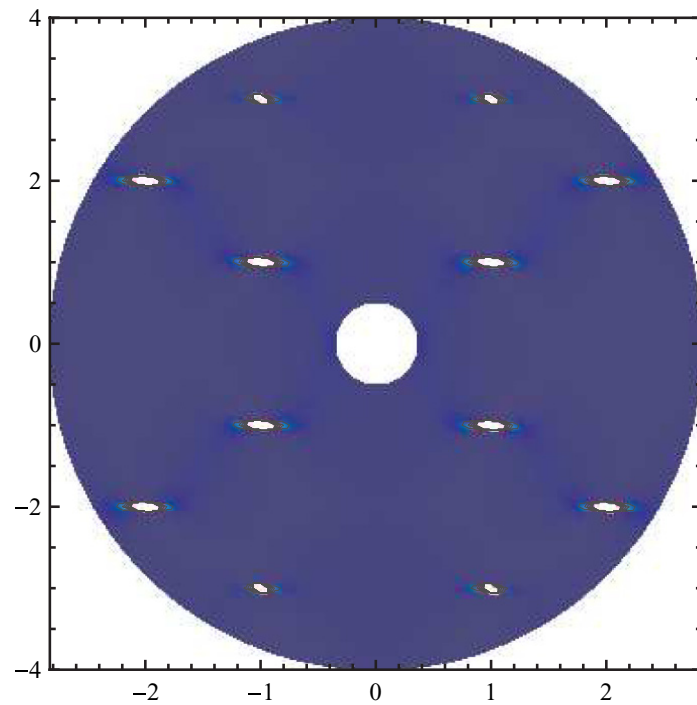


S. Powell, PRB 91,094431 (2015)



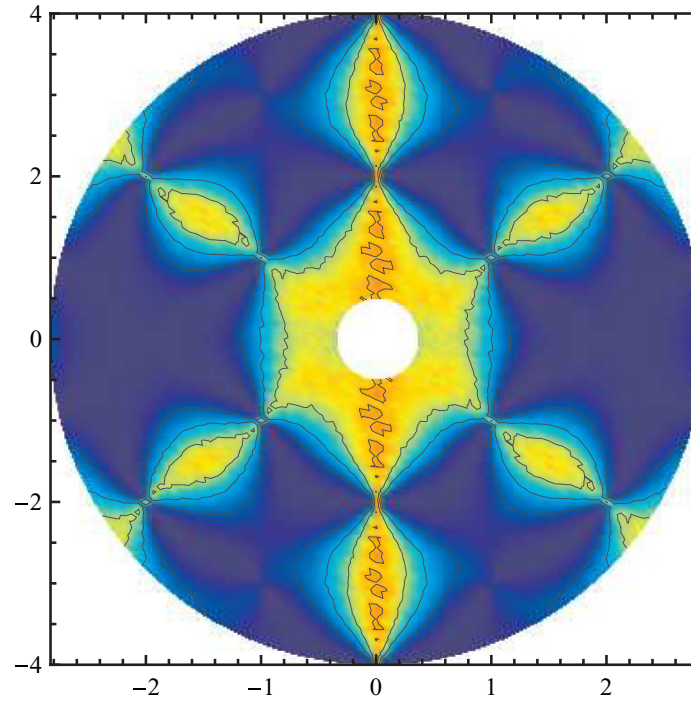
# MAGNETIC MOMENT FRAGMENTATION

Ordered phase



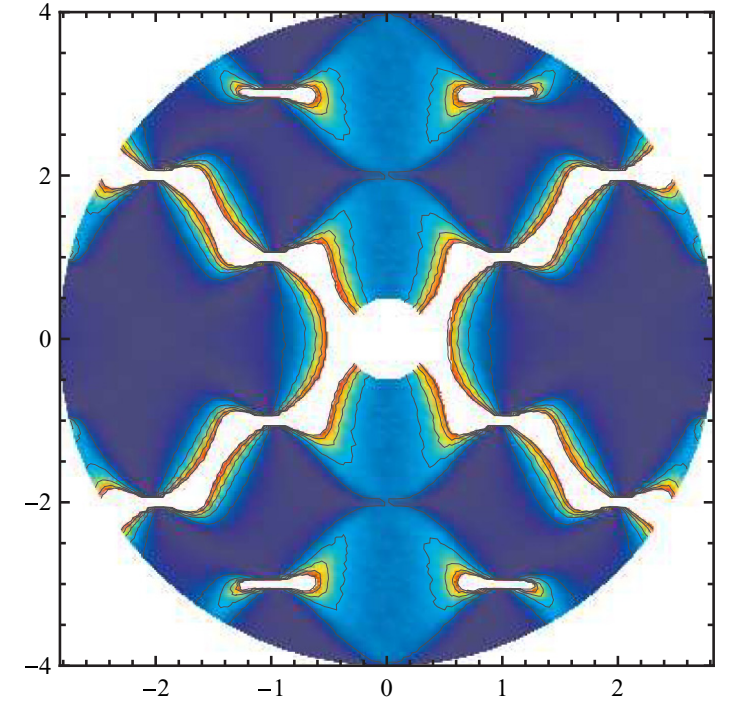
+

Cooperative paramagnet



=

Fragmentation



S. Powell, PRB 91,094431 (2015)

# MAGNETIC MOMENT FRAGMENTATION

PRL **108**, 037202 (2012)

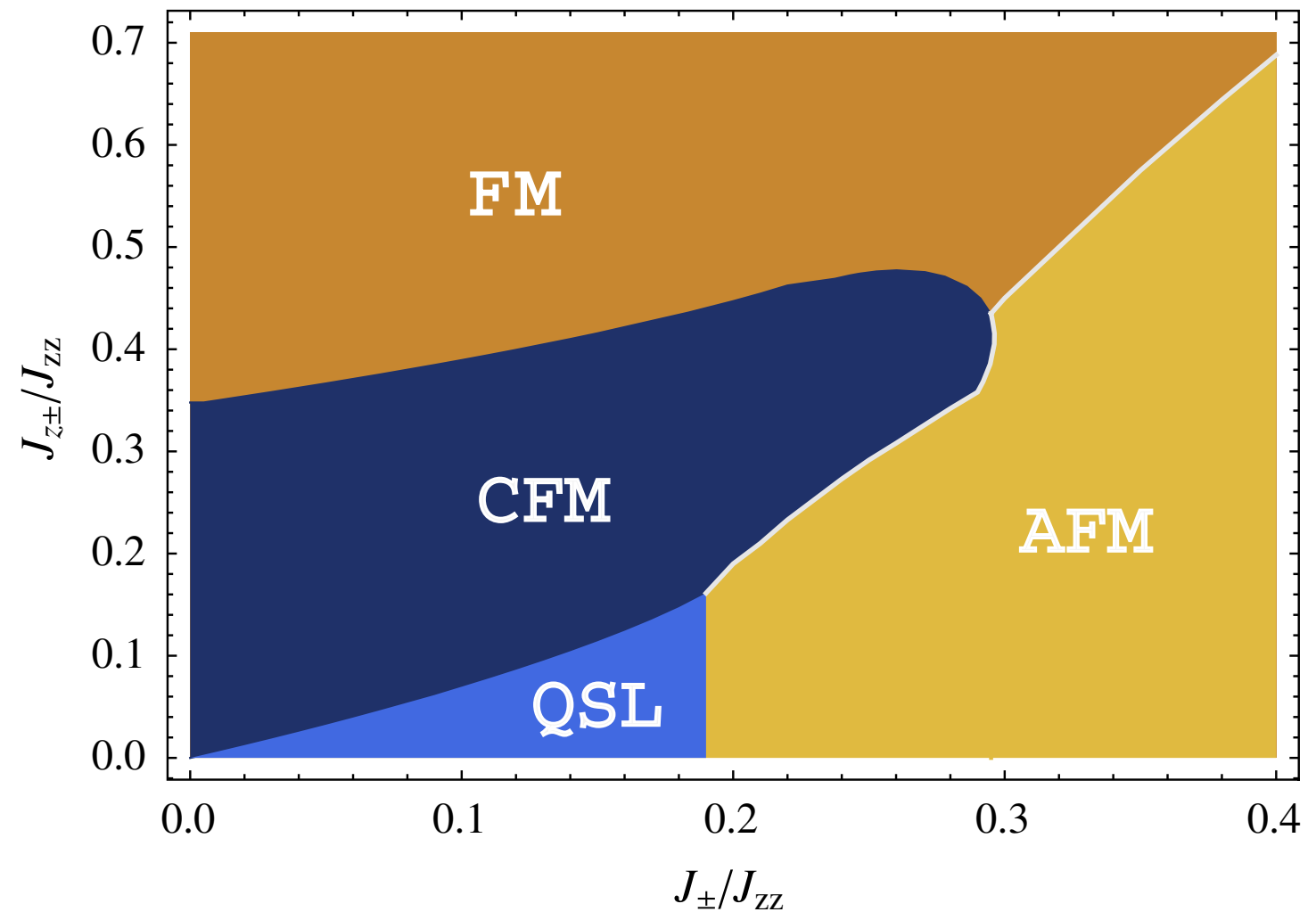
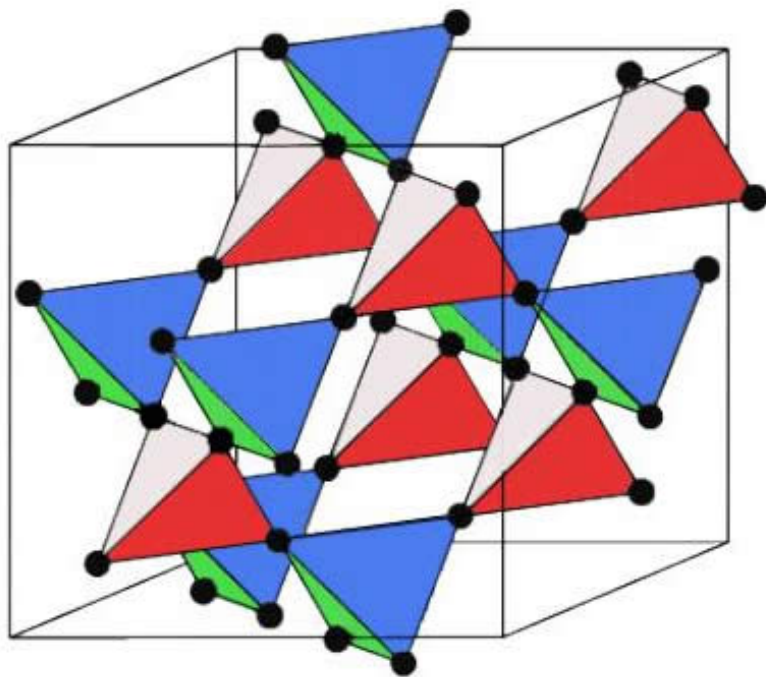
PHYSICAL REVIEW LETTERS

week ending  
20 JANUARY 2012

## Coulombic Quantum Liquids in Spin-1/2 Pyrochlores

Lucile Savary<sup>1,2</sup> and Leon Balents<sup>3</sup>

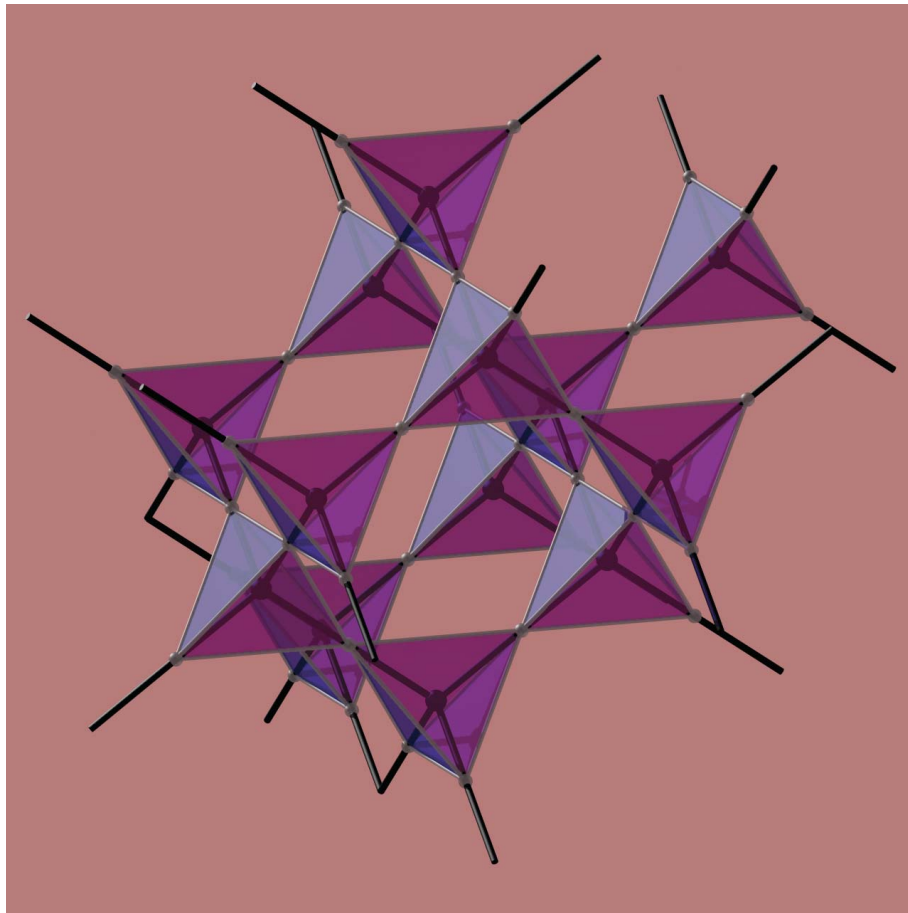
$$H = \sum_{\langle ij \rangle} \{ J_{zz} S_i^z S_j^z - J_{\pm} (S_i^+ S_j^- + S_i^- S_j^+) \\ + J_{\pm\pm} [\gamma_{ij} S_i^+ S_j^+ + \gamma_{ij}^* S_i^- S_j^-] \\ + J_{z\pm} [S_i^z (\zeta_{ij} S_j^+ + \zeta_{ij}^* S_j^-) + i \leftrightarrow j] \},$$



# Magnetic monopoles in spin ice

Vol 451 | 3 January 2008 | doi:10.1038/nature06433

C. Castelnovo<sup>1</sup>, R. Moessner<sup>1,2</sup> & S. L. Sondhi<sup>3</sup>



$$V(r_{\alpha\beta}) = \begin{cases} \frac{\mu_0}{4\pi} \frac{Q_\alpha Q_\beta}{r_{\alpha\beta}} & \alpha \neq \beta \\ \frac{1}{2} v_0 Q_\alpha^2 & \alpha = \beta \end{cases}$$

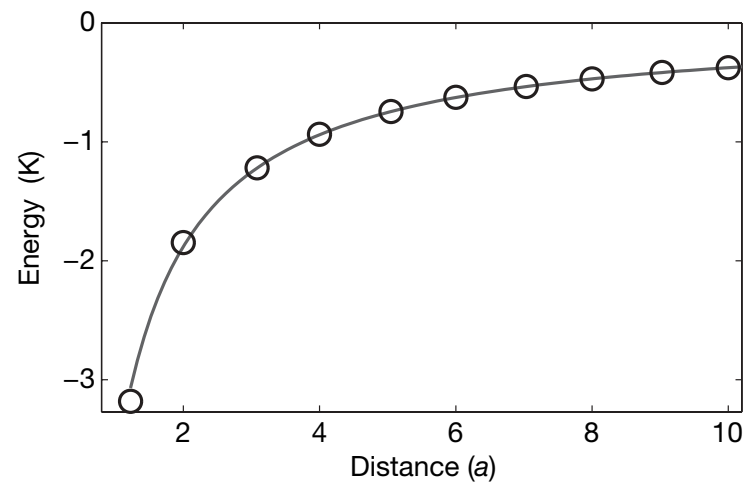


**Figure 3 | Monopole interaction.** Comparison of the magnetic Coulomb energy  $-\mu_0 q_m^2 / (4\pi r)$  (equation (2); solid line) with a direct numerical evaluation of the monopole interaction energy in dipolar spin ice (equation (1); open circles), for a given spin-ice configuration (Fig. 2e), as a function of monopole separation.

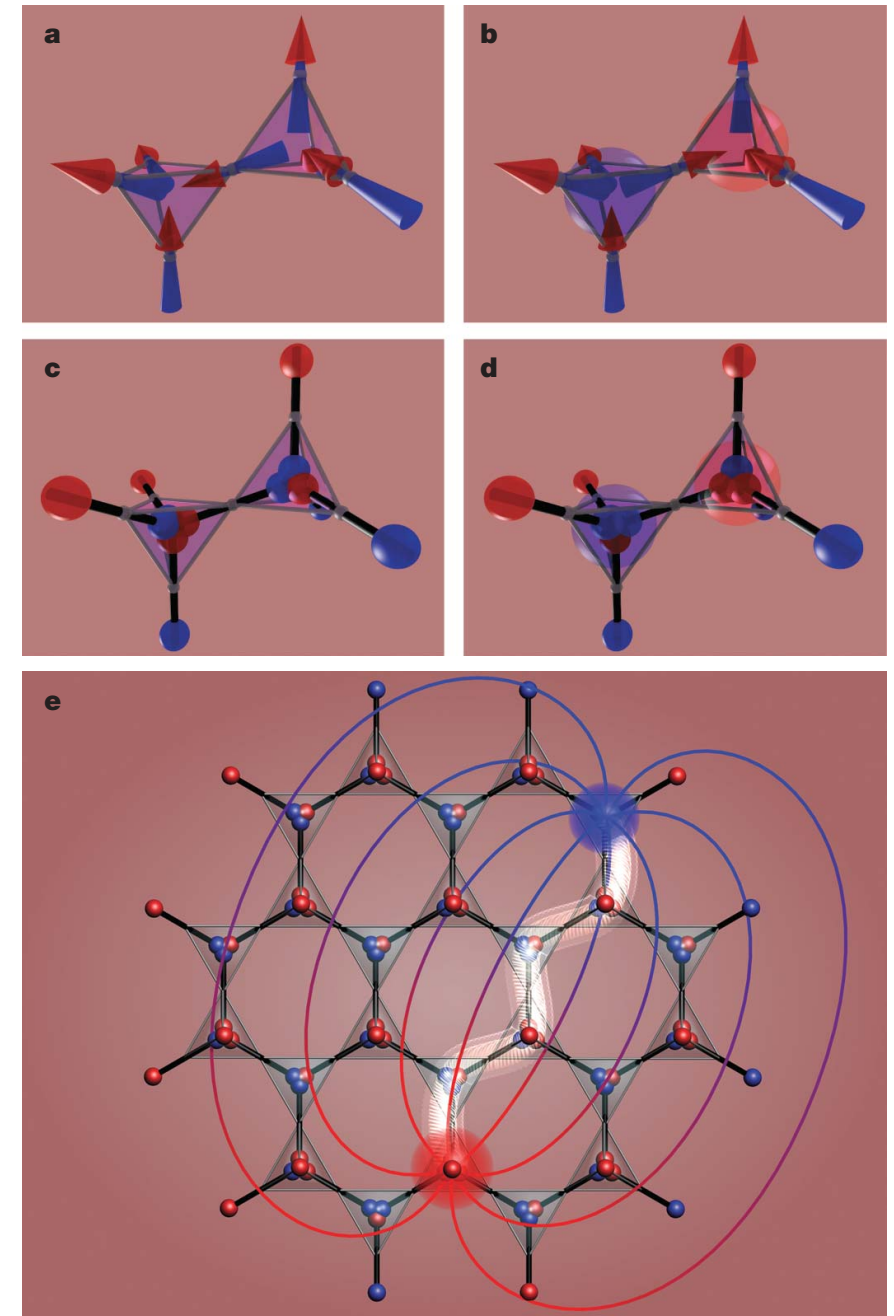


**Figure 2 | Mapping from dipoles to dumbbells.** The dumbbell picture (c, d) is obtained by replacing each spin in a and b by a pair of opposite magnetic charges placed on the adjacent sites of the diamond lattice. In the left panels (a, c), two neighbouring tetrahedra obey the ice rule, with two spins pointing in and two out, giving zero net charge on each site. In the right panels (b, d), inverting the shared spin generates a pair of magnetic monopoles (diamond sites with net magnetic charge). This configuration has a higher net magnetic moment and it is favoured by an applied magnetic field oriented upward (corresponding to a [111] direction). e, A pair of separated monopoles (large red and blue spheres). A chain of inverted dipoles ('Dirac string') between them is highlighted in white, and the magnetic field lines are sketched.



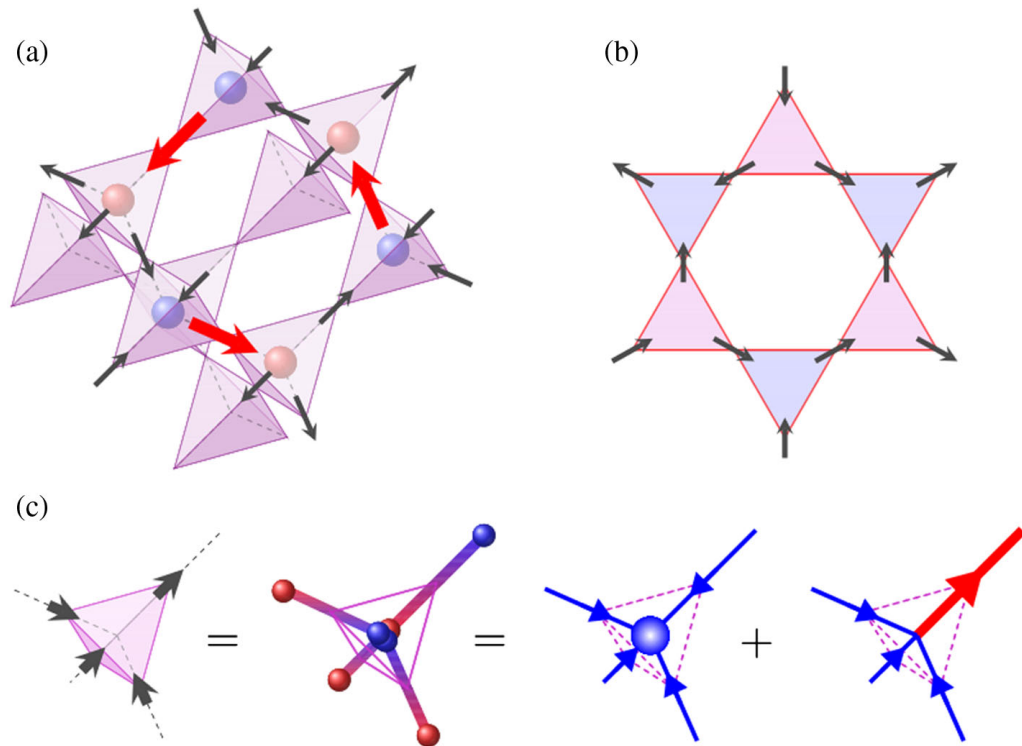
# Magnetic-Moment Fragmentation and Monopole Crystallization

M. E. Brooks-Bartlett,<sup>1</sup> S. T. Banks,<sup>1</sup> L. D. C. Jaubert,<sup>2</sup> A. Harman-Clarke,<sup>1,3</sup> and P. C. W. Holdsworth<sup>3,\*</sup>

monopole density or of monopole ordering [12]. We introduce the concept of magnetic-moment fragmentation, whereby the magnetic-moment field undergoes a novel form of fractionalization into two parts: a divergence-full part representing magnetic monopoles and a divergence-free part corresponding to the emergent Coulomb phase with independent and ergodic spin fluctuations [13]. Our

The divergence in  $\vec{H}$  is related to the breaking of the ice rules through  $\vec{M}$ , the magnetic-moment density that itself obeys Gauss's law  $\vec{\nabla} \cdot \vec{M} = -\rho_m$ . This constraint does

$$\vec{M} = \vec{M}_m + \vec{M}_d = \vec{\nabla} \psi(r) + \vec{\nabla} \wedge \vec{Q}.$$



$$[M_{ij}] \begin{pmatrix} a \\ m \end{pmatrix} = (-1, -1, -1, 1) = \left(-\frac{1}{2}, -\frac{1}{2}, -\frac{1}{2}, -\frac{1}{2}\right) + \left(-\frac{1}{2}, -\frac{1}{2}, -\frac{1}{2}, \frac{3}{2}\right). \quad (2)$$

# Magnetic-Moment Fragmentation and Monopole Crystallization

M. E. Brooks-Bartlett,<sup>1</sup> S. T. Banks,<sup>1</sup> L. D. C. Jaubert,<sup>2</sup> A. Harman-Clarke,<sup>1,3</sup> and P. C. W. Holdsworth<sup>3,\*</sup>

For an ideally ordered array, the divergence-free fields on alternate sites are perfectly satisfied by the sets  $[M_{ij}]_d = +(-)(m/a)(1/2, 1/2, 1/2, -3/2)$ . Thus, one sees the emergence of a new Coulomb phase with extensive entropy superimposed on monopole order, in which each vertex has three contributions to the dipolar field of strength  $1/2$  [in units of  $(m/a)$ ] and one of strength  $3/2$ , which is shared between a pair of neighboring sites on opposite sublattices. This fragmented state could be termed an “antiferromagnetic Coulomb magnet” by analogy with the “ferromagnetic Coulomb magnet,” predicted in the gauge mean-field theory of quantum magnets on a pyrochlore lattice [25]. The ordered component corresponds to a broken symmetry of the Ising spins described in the local-axis reference frame into the three-up–one-down or three-down–one-up sector. For the divergence-free part  $\vec{M}_d$ , placing a dimer along the bond of strength  $3/2$  provides a mapping between the emergent dipolar field and hard-core dimers on the (bipartite) diamond lattice [26]. The extensive entropy of the dipolar field is thus associated with closed loops of dimer moves [27]. Introducing quantum-loop dynamics gives rise to a U(1) liquid phase close to the Rokhsar-Kivelson point [28,29].

A monopole-crystal ground state can be induced in the dumbbell model by modifying the chemical potential so that the total Coulomb energy  $U_C$  outweighs the energy cost for creating the particles  $-\mu N$ . For the monopolar crystal

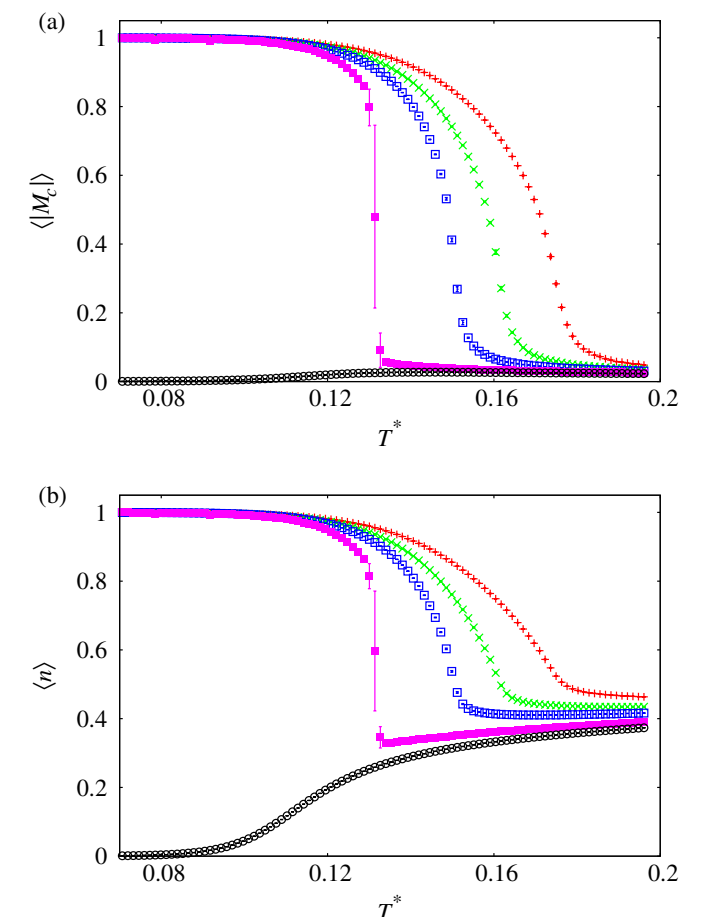
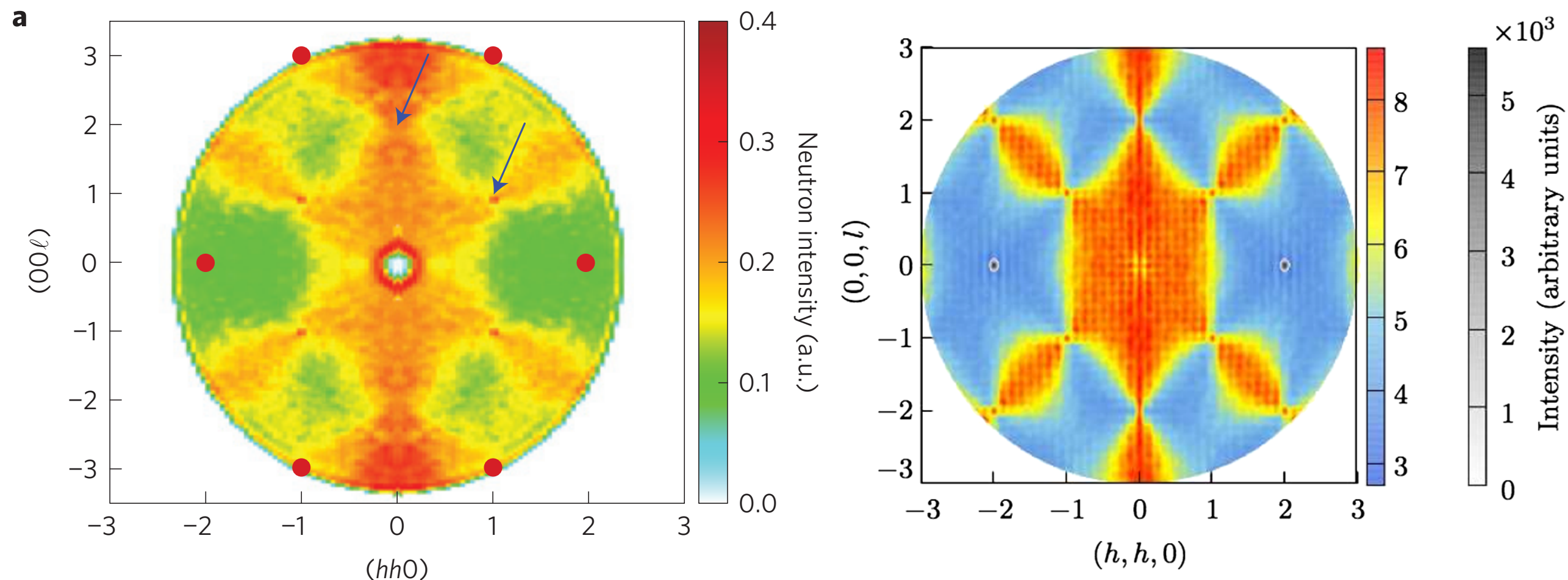


FIG. 2. (a) Order parameter  $M_c$  for monopole crystallization, as defined in Eq. (4), and (b) density of charges  $n$ , as a function of reduced temperature  $T^*$  for chemical potential  $\mu^* = 0.767$  (+),  $0.778$  (x),  $0.784$  (□),  $0.794$  (■), and  $0.801$  (○). The transition appears to pass from second order to first order via a tricritical point for  $\mu_{tr}^* \approx 0.78$ . The very narrow first-order region ends at  $\mu^* \approx 0.80$ , above which spin-ice physics is recovered (e.g., the open black circles). The alternating positive or negative charges on the diamond lattice can also be seen as stacked monolayers of monopoles of the same charge in all three cubic directions. Note that the configurational constraints of the singly charged monopole fluid result in a high-temperature limit for the density of  $n = 4/7$ , rather than the  $n = 0.5$  expected for an unconstrained bipartite lattice gas. A generalization of the worm algorithm has been developed to ensure equilibration at low temperature (Appendix B).

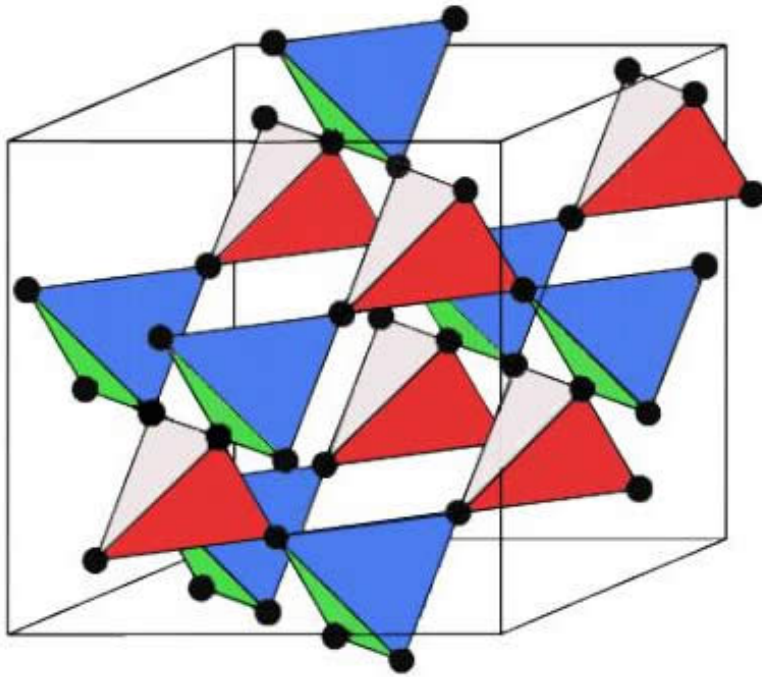
# Observation of magnetic fragmentation in spin ice

S. Petit<sup>1\*</sup>, E. Lhotel<sup>2\*</sup>, B. Canals<sup>2</sup>, M. Ciomaga Hatnean<sup>3</sup>, J. Ollivier<sup>4</sup>, H. Mutka<sup>4</sup>, E. Ressouche<sup>5</sup>,  
A. R. Wildes<sup>4</sup>, M. R. Lees<sup>3</sup> and G. Balakrishnan<sup>3</sup>



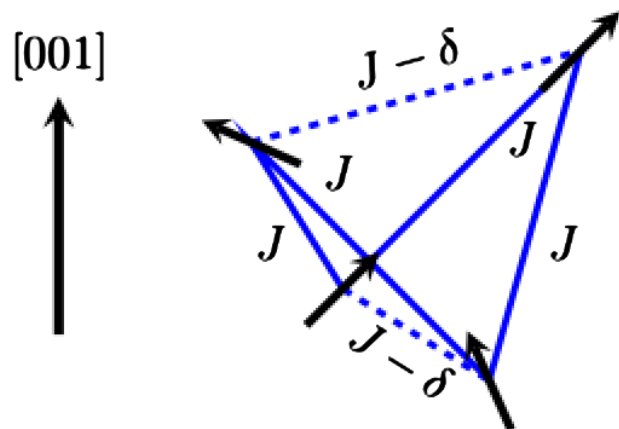
# Spin Ice under Pressure: Symmetry Enhancement and Infinite Order Multicriticality

L. D. C. Jaubert,<sup>1</sup> J. T. Chalker,<sup>2</sup> P. C. W. Holdsworth,<sup>3</sup> and R. Moessner<sup>1</sup>

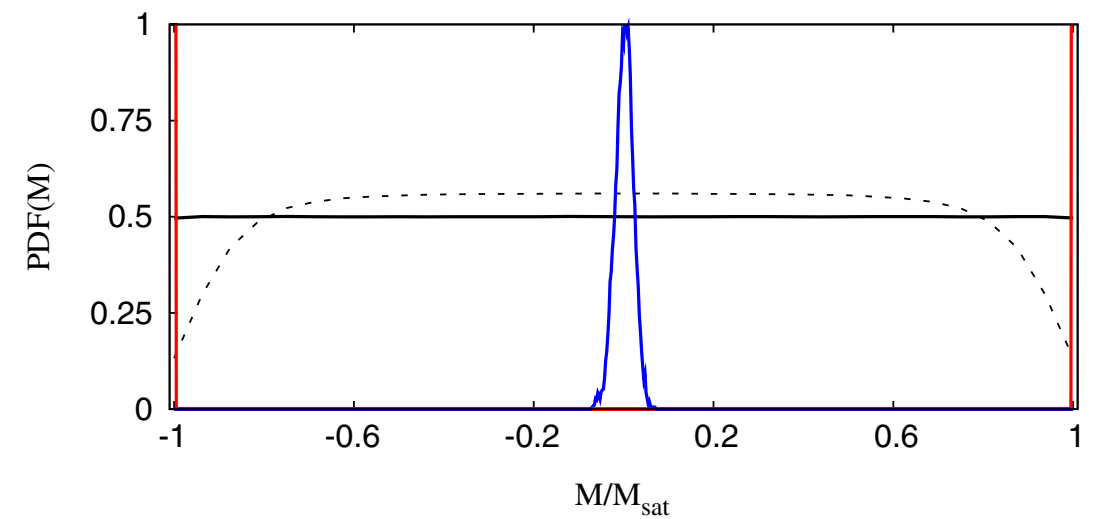
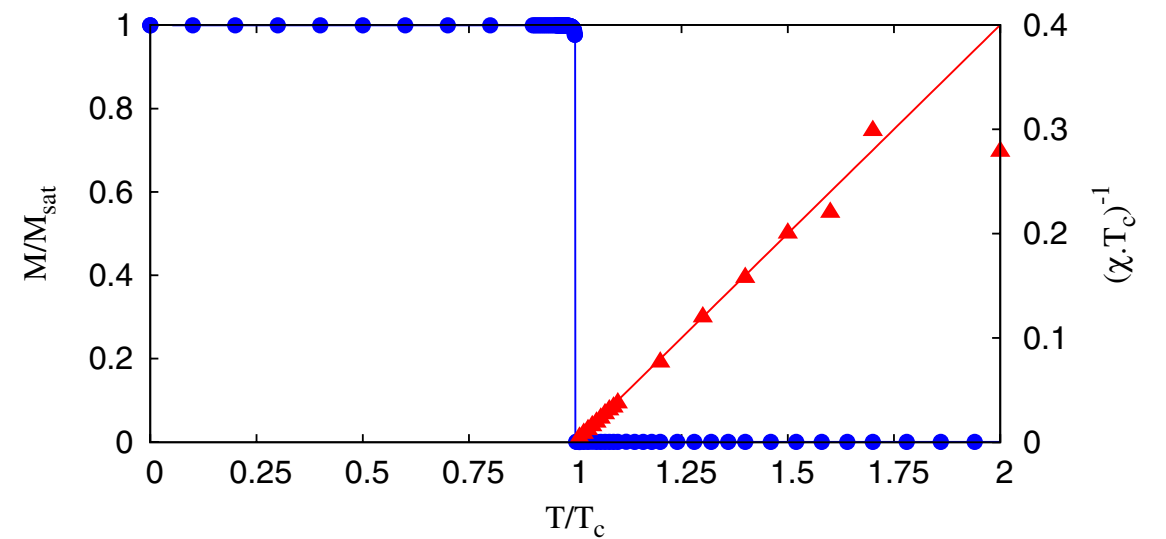


$$\mathcal{H} = -\sum_{\langle i,j \rangle} J_{ij} \mathbf{S}_i \cdot \mathbf{S}_j, \quad (1)$$

where  $J_{ij} = J - \delta > 0$  for bonds on (001) planes perpendicular to the strain axis, and  $J_{ij} = J$  otherwise (see Fig. 1).

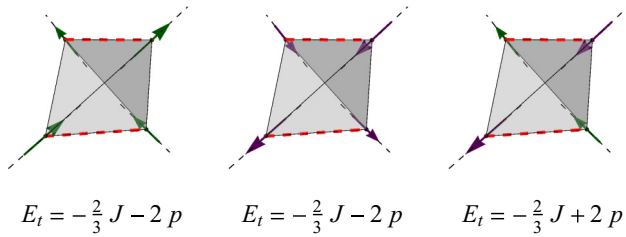


$$G(M) = \frac{a}{2} (T - T_c) M^2 + \frac{b}{2n} M^{2n}. \quad (2)$$



# Ferromagnetic Coulomb phase in classical spin ice

Stephen Powell



Given the magnetization-independent free energy at the transition, it is clear that any perturbation that produces a positive fourth-order coefficient in the Landau function should lead to an intermediate phase with  $0 < |M_z| < M_{\text{sat}}$ . While this argument does not provide a prescription for constructing appropriate perturbations, one expects on general grounds that a sufficiently long-ranged four-spin interaction will have this effect. (As will also be demonstrated, a quartic coefficient with opposite sign should lead to a first-order transition.)

$$\mathcal{H}_{\text{nn}} = - \sum_{\langle ij \rangle} J_{ij} \mathbf{S}_i \cdot \mathbf{S}_j ,$$

$$\mathcal{H}_{4\text{s}} = V_4 \sum_{\{tt'\}} [\Theta_+(\mathbf{S}_t, \mathbf{S}_{t'}) + \Theta_-(\mathbf{S}_t, \mathbf{S}_{t'})] , \quad (3)$$

$$\Theta_{\pm}(\mathbf{S}, \mathbf{S}') = \begin{cases} 1 & \text{if } \mathbf{S} = \mathbf{S}' = \pm \frac{4}{\sqrt{3}} \hat{\mathbf{z}} \\ 0 & \text{otherwise} \end{cases} \quad (4)$$

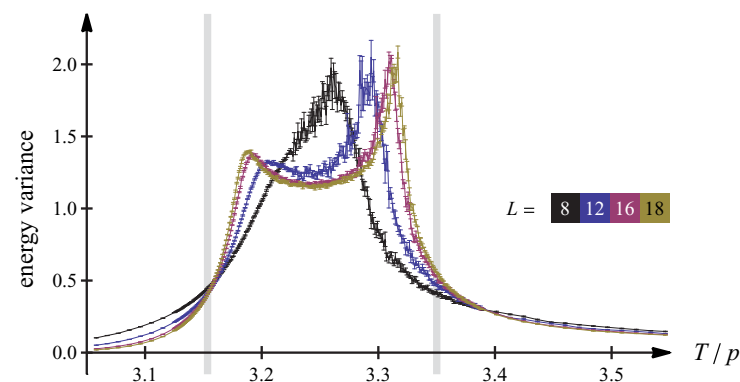
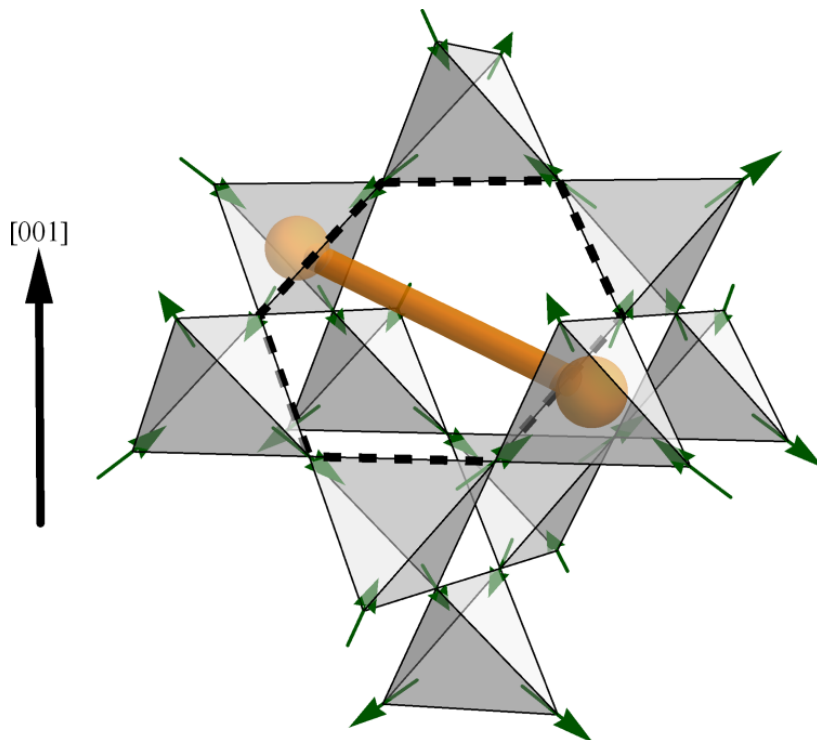
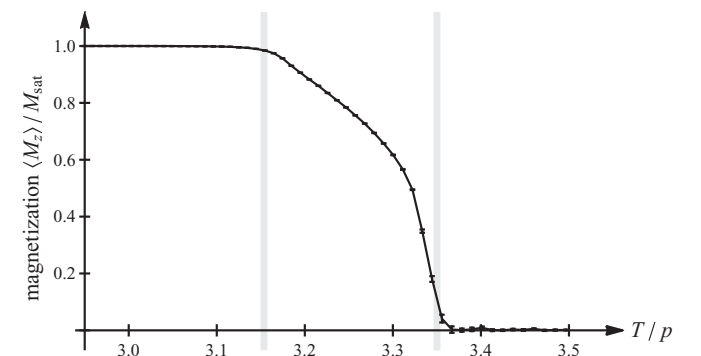
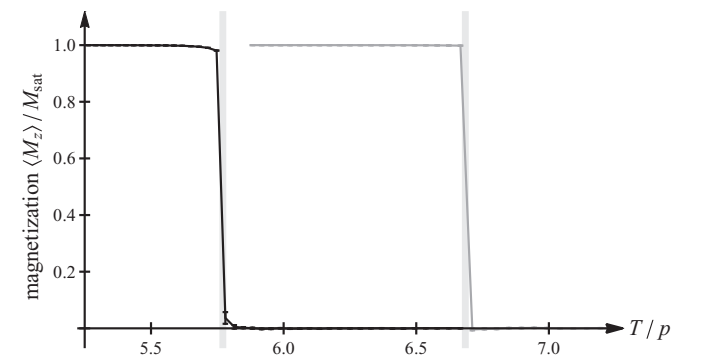


FIG. 5. (Color online) Variance of energy,  $(\langle E^2 \rangle - \langle E \rangle^2)/N_s$ , vs temperature for fixed  $V_4/T = 0.05$  and various system sizes. The vertical lines indicate the positions of phase transitions in the thermodynamic limit (determined by other means). The double-peak structure, with peak heights at most weakly diverging with  $L$ , is consistent with a pair of continuous transitions.





# Ferromagnetic Coulomb phase in classical spin ice

Stephen Powell

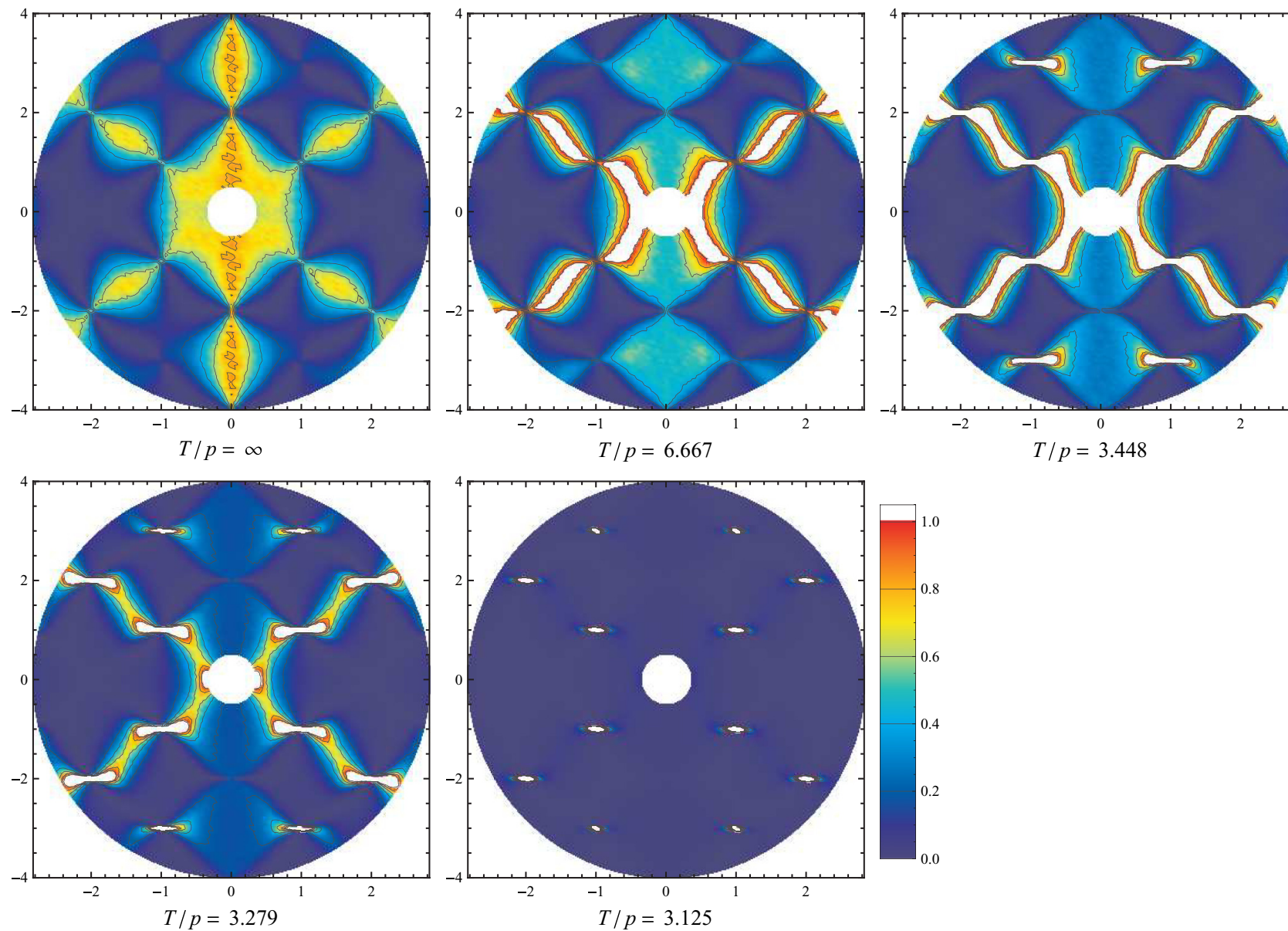


FIG. 10. (Color online) Structure factor for (spin-flip) polarized neutron scattering [17]  $S_{\text{SF}}(\mathbf{Q})$ , defined in Eq. (5), for scattering wave vector  $\mathbf{Q}$  in the  $(h\ell\ell)$  plane and incident polarization  $\mathbf{P}$  along  $[1\bar{1}0]$ . The first three plots are for temperatures above  $T_{\infty}$ , the fourth is in the intermediate phase,  $T_{c<} < T < T_{c>}$ , and the last is below  $T_{c<}$ . Pinch points, characteristic of the dipolar correlations of the Coulomb phase, are visible at all temperatures but the lowest. In the intermediate phase, there are also Bragg peaks at certain reciprocal-lattice vectors, indicating spontaneous magnetization. The system size is  $L = 16$  and all plots have  $V_4/T = 0.05$ . (Wave vectors are measured in units corresponding to the conventional cubic unit cell.)

# **PART 2 – FRUSTRATED ARRAYS OF JOSEPHSON JUNCTIONS**

## Pairing of Cooper Pairs in a Fully Frustrated Josephson-Junction Chain

Benoit Douçot<sup>1,2</sup> and Julien Vidal<sup>3</sup>

white circles in Fig. 1. The system is described by the following Josephson coupling Hamiltonian:

$$H_J = -t_J \sum_n a_n^\dagger (b_n + c_n + b_{n-1} + e^{-i\gamma} c_{n-1}) + \text{H.c.} \quad (1)$$

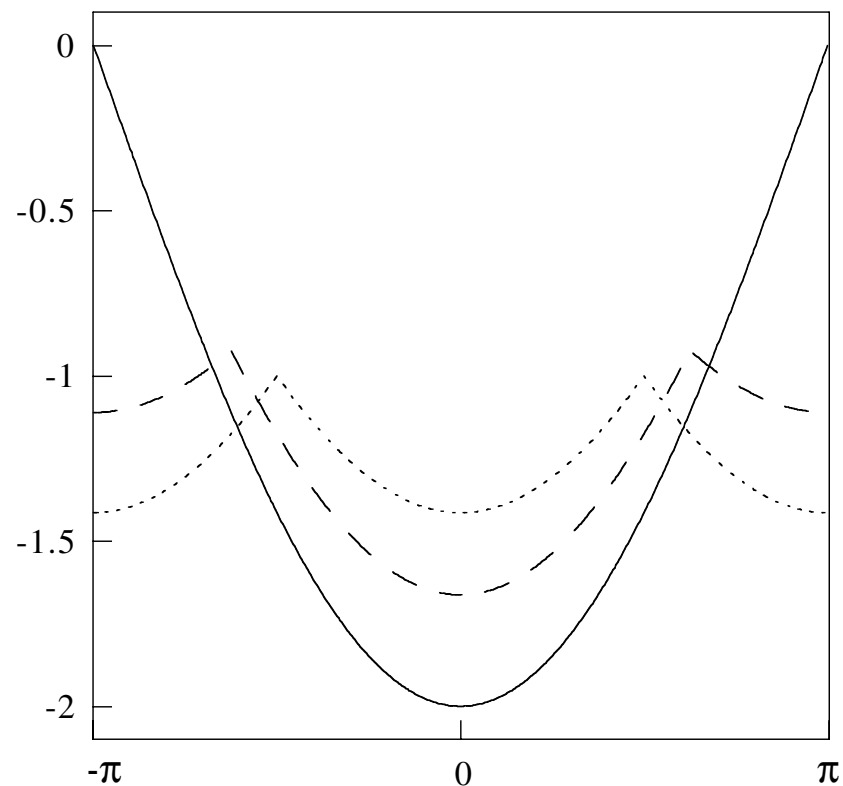


FIG. 2. Behavior of  $F(x_n)$  for  $\gamma = 0$  (solid line),  $\gamma = 3\pi/4$  (dashed line), and  $\gamma = \pi$  (dotted line).

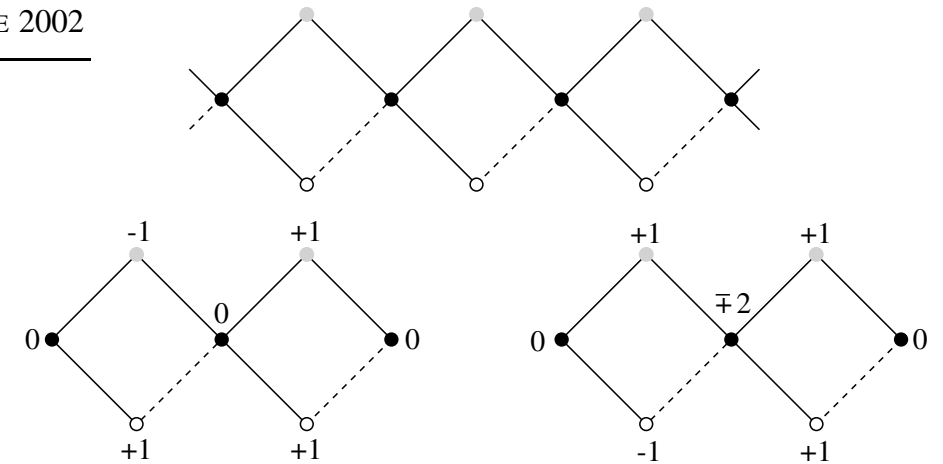


FIG. 1. The chain of loops and the three (non-normalized) cage eigenstates corresponding to  $\varepsilon_0$  (left) and  $\varepsilon_{\pm}$  (right). The dashed lines symbolize the hopping term  $-t_J e^{-i\gamma}$ .

$$\mathcal{H} = -\frac{1}{2} \sum_{\langle ij \rangle} \cos(\varphi_i - \varphi_j - \alpha_{ij})$$

$$C_p(n) = \langle \cos(p(\varphi_{i+n} - \varphi_i)) \rangle$$

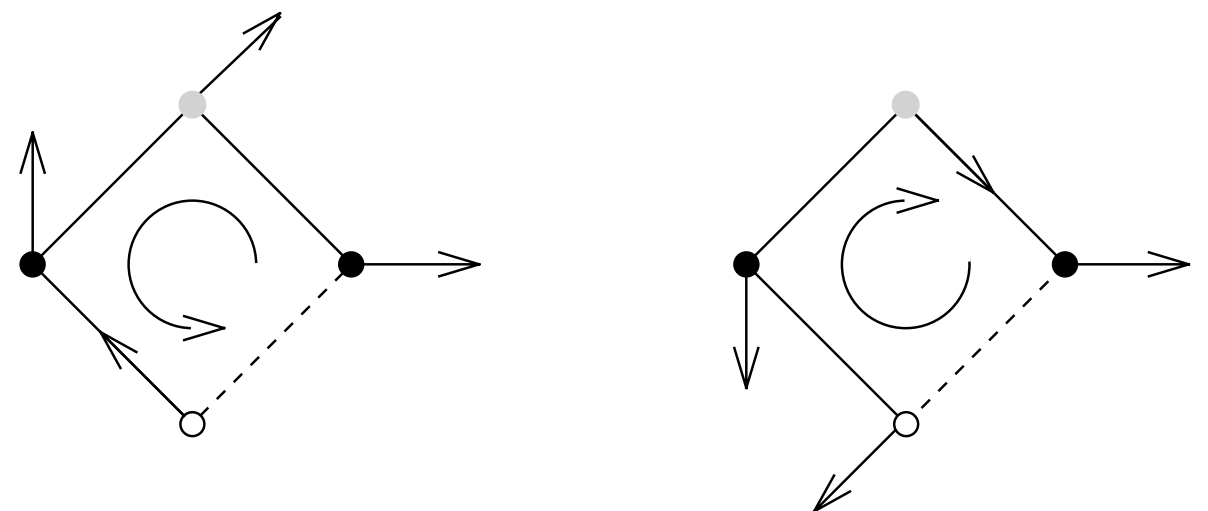


FIG. 3. Two possible classical ground states of  $H$  with different chirality.



# FRUSTRATED ARRAYS OF JOSEPHSON JUNCTIONS

PHYSICAL REVIEW B **66**, 144502 (2002)

PHYSICAL REVIEW B

VOLUME 55, NUMBER 17

1 MAY 1997-I

## Ground states of a frustrated kagomé array of Josephson junctions

Mohammad R. Kolahchi<sup>1</sup> and Joseph P. Straley<sup>2</sup>

<sup>1</sup>*Institute for Advanced Studies in Basic Sciences, Gava Zang, P. O. Box 45195-159, Zanjan, Iran*

<sup>2</sup>*Department of Physics, University of Kentucky, Lexington, Kentucky 40506*

(Received 13 April 2002; revised manuscript received 20 June 2002; published 14 October 2002)

$$\chi_{ij} = \frac{2e}{c\hbar} \int_i^j \vec{A}(\vec{r}) \cdot d\vec{l}. \quad (1)$$

The Hamiltonian is given by

$$H = -J \sum_{\langle ij \rangle} \cos(\theta_i - \theta_j - \chi_{ij}), \quad (2)$$

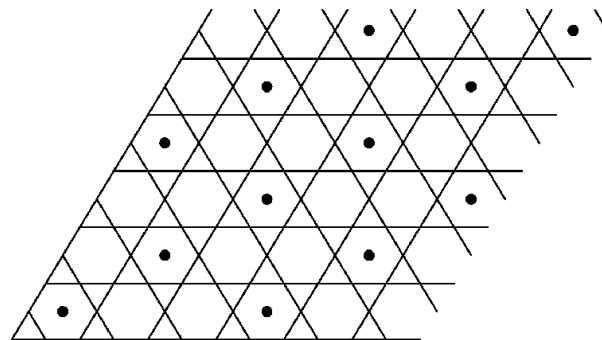


FIG. 5. Vortex arrangement for the ground state for  $f=1/6$ . The triangles are all in the state  $f\# = 0$ , while the hexagons are in states  $F\# = 1$  (with no current on their boundaries) and 2 (with current  $J\sqrt{3}/2$ ). Dots have been drawn in the hexagons with  $F\# = 2$  vorticity.

## Phase transitions in a kagomé lattice of Josephson junctions

M. S. Rzchowski

*Physics Department and Applied Superconductivity Center, University of Wisconsin-Madison, Madison, Wisconsin 53706*

(Received 15 October 1996)

$$H = - \sum_{i,j \in \{NN\}} E_J \cos(\theta_i - \theta_j - A_{ij}), \quad (1)$$

where

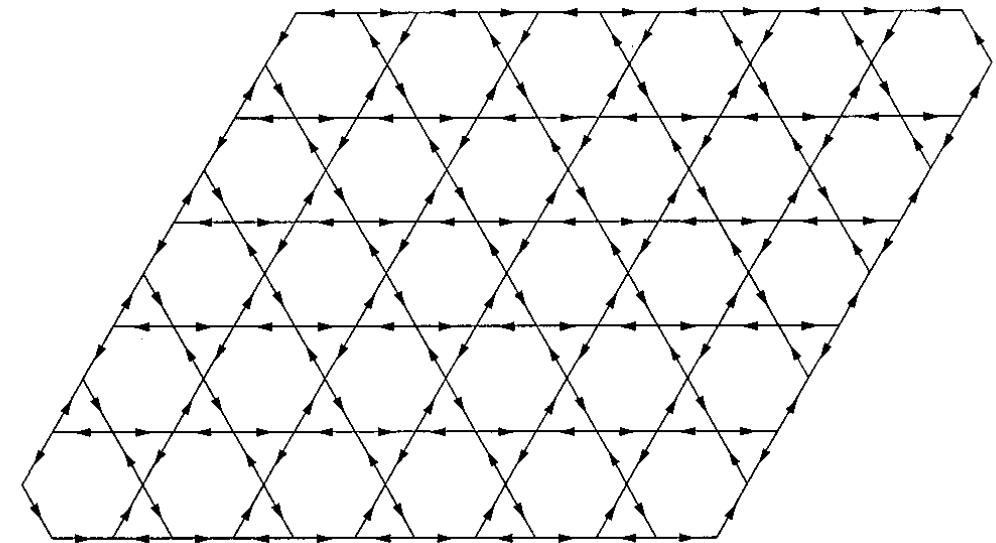
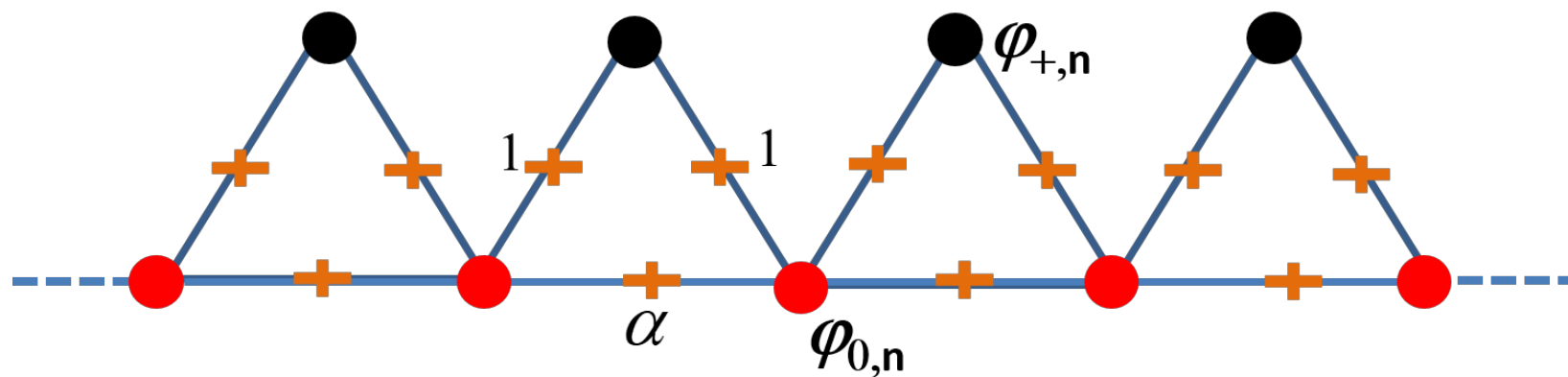


FIG. 1. Schematic representation of the ground states for  $f=0, 1/8, 1/4, 3/8$ , and  $1/2$  for an array of Josephson junctions on a kagomé lattice. The arrows represent the direction of circulating currents. All currents in these ground states are of equal magnitude, unlike other lattices investigated.

# MOTIVATION

- ▶ (classical) arrays of Josephson junctions = frustrated systems
- ▶ Increasing frustration destabilizes ferromagnetic groundstate
- ▶ (Mostly) single point of massive degeneracy
- ▶ Frustration enters as phase shifts:  $\cos(\varphi_i - \varphi_j - A_{ij})$
- ▶ What happens if the couplings are changed?
- ▶  $J_{ij} \cos(\varphi_i - \varphi_j)$

$$\mathcal{H} = -\frac{1}{2} \sum_{\langle ij \rangle} J_{ij} \vec{s}_i \vec{s}_j = -\frac{1}{2} \sum_{\langle ij \rangle} J_{ij} \cos(\varphi_i - \varphi_j)$$

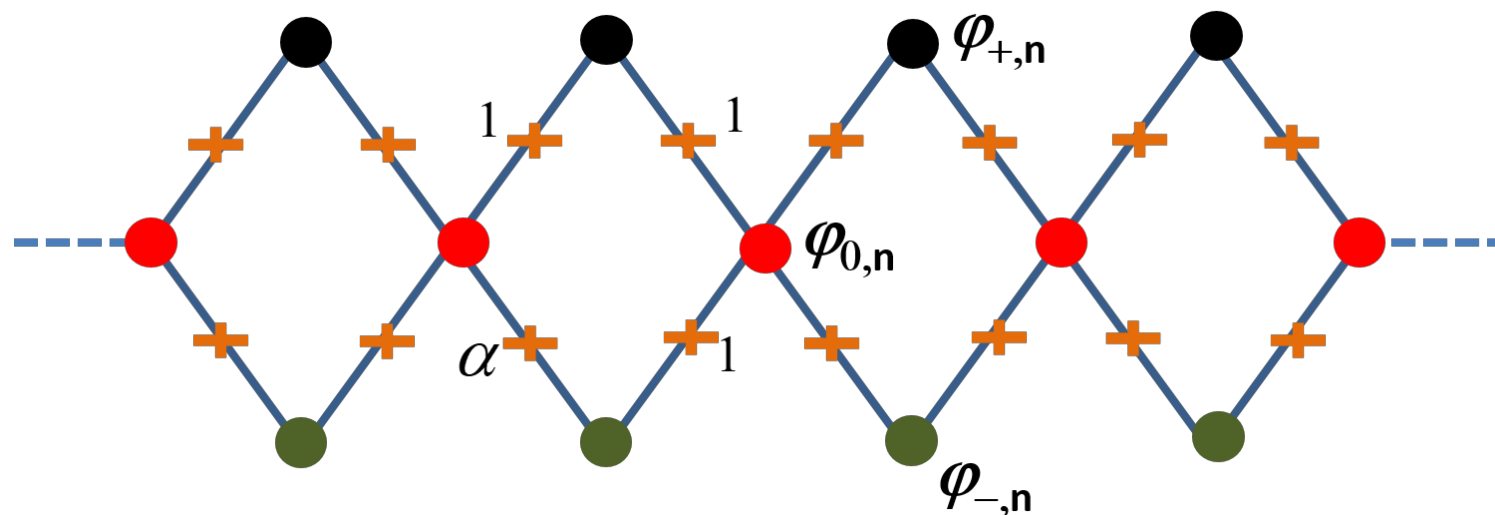


$$J_{ij} = 1, \alpha$$

$$-1 \leq \alpha \leq 1$$

Frustration:

$$f = \frac{1 - \alpha}{2}$$



$$f = 0 \text{ no frustration}$$

$$f = 1 \text{ maximum frustration}$$

# SPIN-WAVE SPECTRUM – DIAMOND CHAIN

Linearise around the uniform groundstate  $f \leq f_c$

$$\frac{1}{\omega_p^2} \ddot{\varphi}_{+,n} = \varphi_{0,n} + \varphi_{0,(n+1)} - 2\varphi_{+,n} , \quad (5)$$

$$\frac{1}{\omega_p^2} \ddot{\varphi}_{-,n} = (1 - 2f)\varphi_{0,n} + \varphi_{0,(n+1)} - 2(1 - f)\varphi_{-,n} ,$$

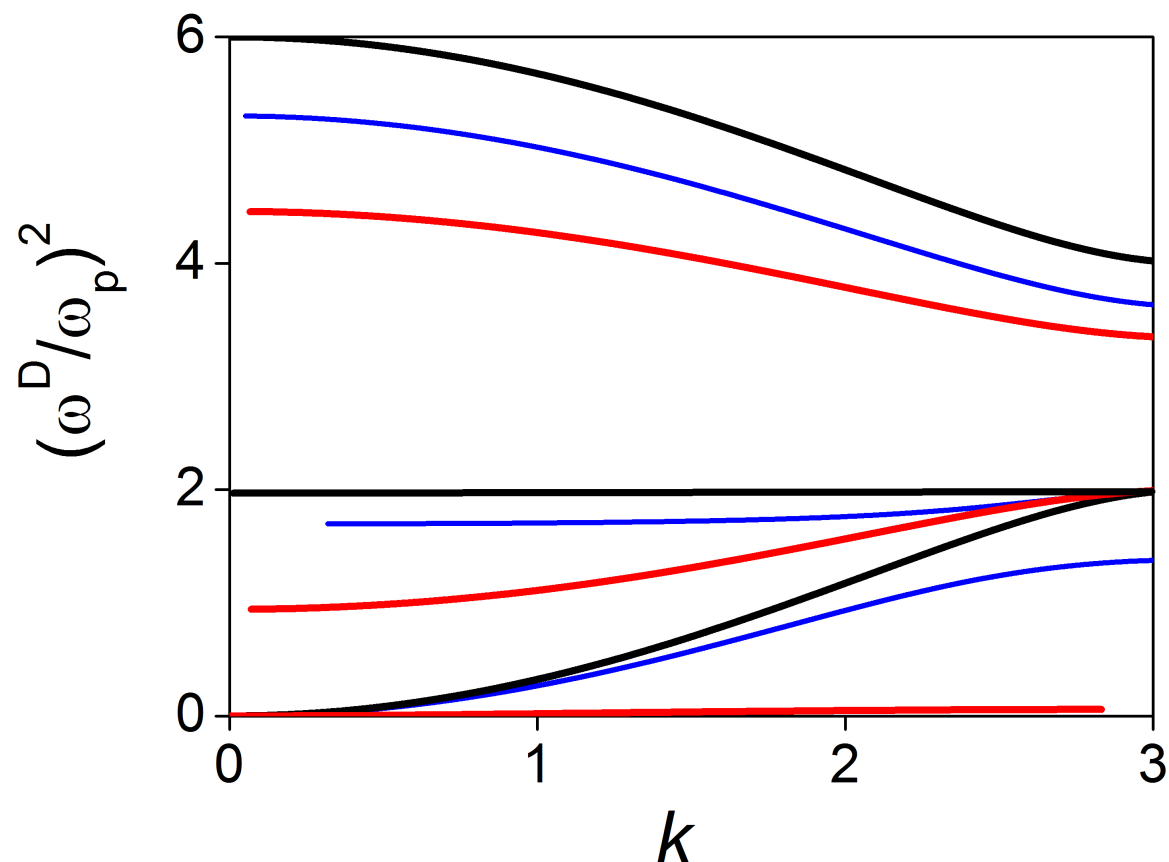
$$\frac{1}{\omega_p^2} \ddot{\varphi}_{0,n} = \varphi_{+,n} + \varphi_{+,(n-1)} + (1 - 2f)\varphi_{-,n}$$

$$+ \varphi_{-,(n-1)} - 2(2 - f)\varphi_{0,n} .$$

$$-\frac{(\omega^D)^2}{\omega_p^2} + 3 + \alpha = \frac{4 \cos^2 \left( \frac{k}{2} \right)}{2 - \omega^2} + \frac{(\alpha - 1)^2 + 4\alpha \cos^2 \left( \frac{k}{2} \right)}{-\omega^2 + 1 + \alpha} \quad (6)$$

$$f = 0, 0.55, 0.65$$

black, blue, red



Linearise around the uniform groundstate

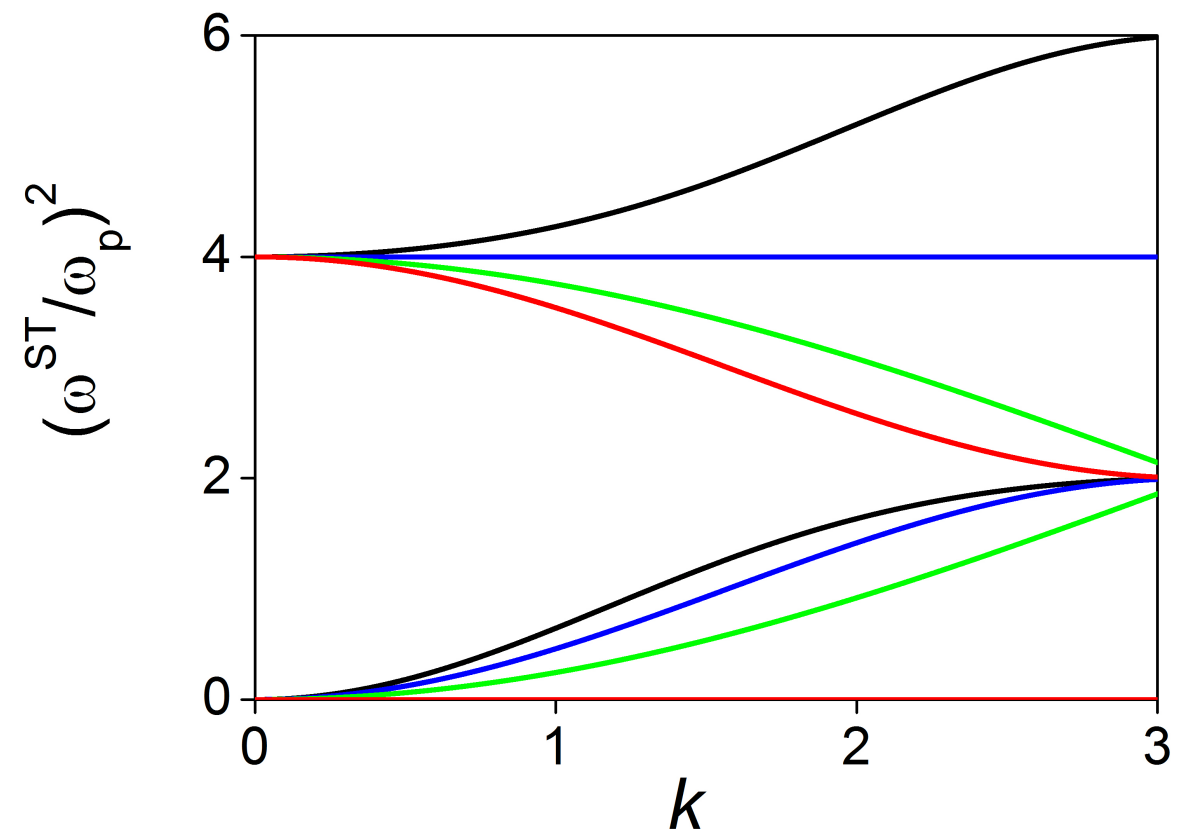
$$f \leq f_c$$

$$\begin{aligned} \frac{1}{\omega_p^2} \ddot{\varphi}_{+,n} &= \varphi_{0,n} + \varphi_{0,(n+1)} - 2\varphi_{+,n} , \\ \frac{1}{\omega_p^2} \ddot{\varphi}_{0,n} &= \varphi_{+,n} + \varphi_{+,(n-1)} + (1-2f)\varphi_{0,n-1} \\ &\quad + (1-2f)\varphi_{0,(n+1)} - 2(1-2f)\varphi_{0,n} . \end{aligned} \quad (7)$$

$$\omega^{ST}(k) = \omega_p \left\{ 2 + 2\alpha \sin^2 \frac{k}{2} \pm \sqrt{4\alpha^2 \sin^4 \frac{k}{2} + 4 \cos^2 \frac{k}{2}} \right\}^{1/2} \quad (8)$$

$$f = 0, 0.25, 0.5, 0.75$$

black,blue,green,red



Unlike most previously studied models, degeneracy persists for a range of frustrations

# Chiral classical states in a rhombus and a rhombi chain of Josephson junctions with two-band superconducting elements

R. G. Dias and A. M. Marques

*Department of Physics & I3N, University of Aveiro, 3810-193 Aveiro, Portugal*

B. C. Coutinho

*Center for Complex Networks Research, Northeastern University, Boston, Massachusetts 02115, USA*

L. P. Martins

*CERN, Geneva 23, CH-1211, Switzerland*

(Received 28 December 2012; revised manuscript received 27 February 2014; published 21 April 2014)

We present a study of Josephson junctions arrays with two-band superconducting elements in the high-capacitance limit. We consider two particular geometries for these arrays: a single rhombus and a rhombi chain with two-band superconducting elements at the spinal positions. We show that the rhombus shaped JJ circuit and the rhombi chain can be mapped onto a triangular JJ circuit and a JJ two-leg ladder, respectively, with zero effective magnetic flux, but with Josephson couplings that are magnetic flux dependent. If the two-band superconductors are in a sign-reversed pairing state, one observes transitions to or from chiral phase configurations in the mapped superconducting arrays when magnetic flux or temperature are varied. The phase diagram for these chiral configurations is discussed. When half-flux quantum threads each rhombus plaquette, new phase configurations of the rhombi chain appear that are characterized by the doubling of the periodicity of the energy density along the chain, with every other two-band superconductor locked in a sign-reversed state. In the case of identical Josephson couplings, the energy of these phase configurations becomes independent of the inner flux in the rhombi chain and the supercurrent along the rhombi chain is zero.

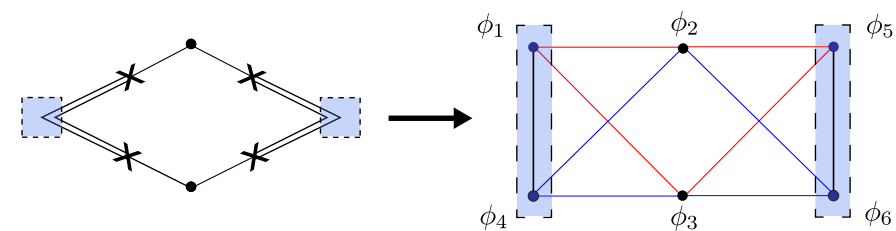
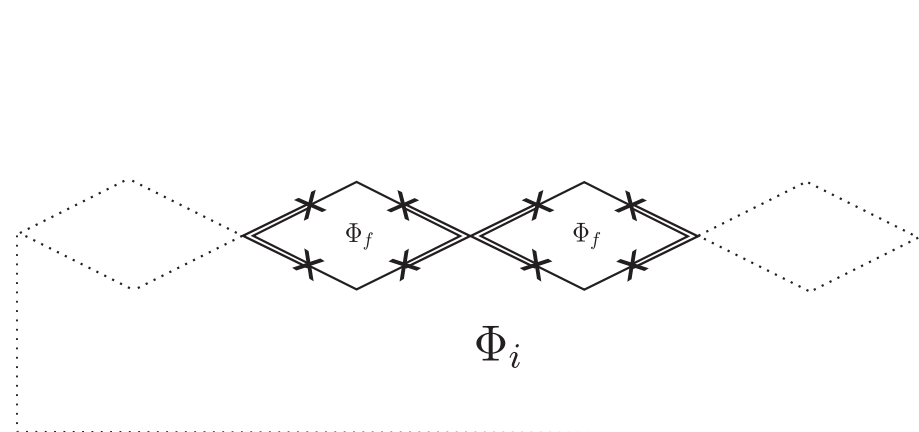
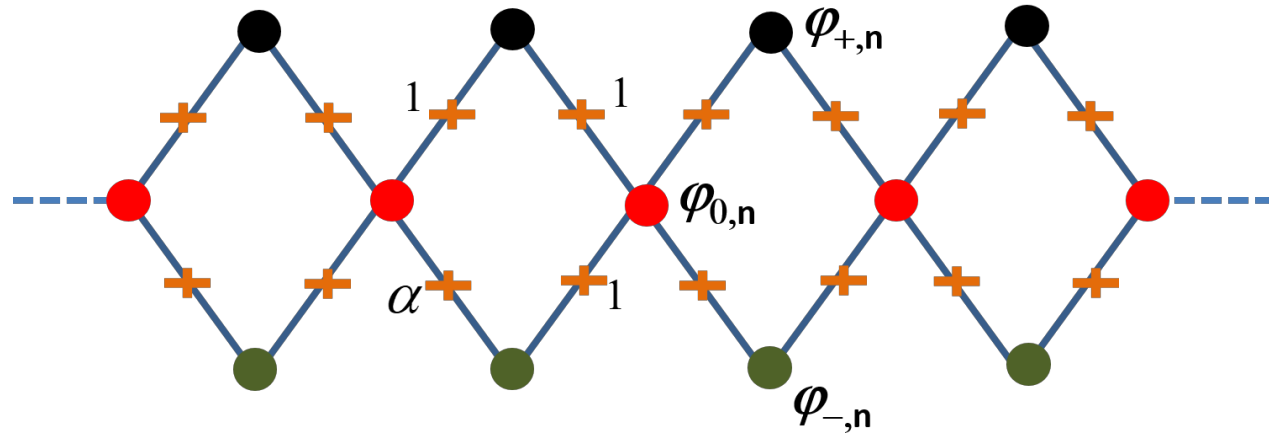


FIG. 2. (Color online) The rhombi chain displayed in Fig. 1 can be considered as equivalent to a JJ two-leg ladder of one-band superconductors with diagonal tunnellings, if one interprets the two bands of the two-band superconductors as two sites of the JJ ladder. In this figure, the dots indicate the superconducting elements, the two-band superconductors are shown as blue dashed boxes (one dot per band) and the segments indicate the Josephson tunnellings.

# DEGENERATE GROUNDSTATE AND CORRELATIONS

25



$$C_p(n) = \langle \cos(p(\varphi_n - \varphi_0)) \rangle$$

$$Z = \int_{\varphi} \exp(-\beta \mathcal{H})$$

$$\mathcal{H} = -\frac{1}{2} \sum_{\langle ij \rangle} J_{ij} \cos(\varphi_i - \varphi_j)$$

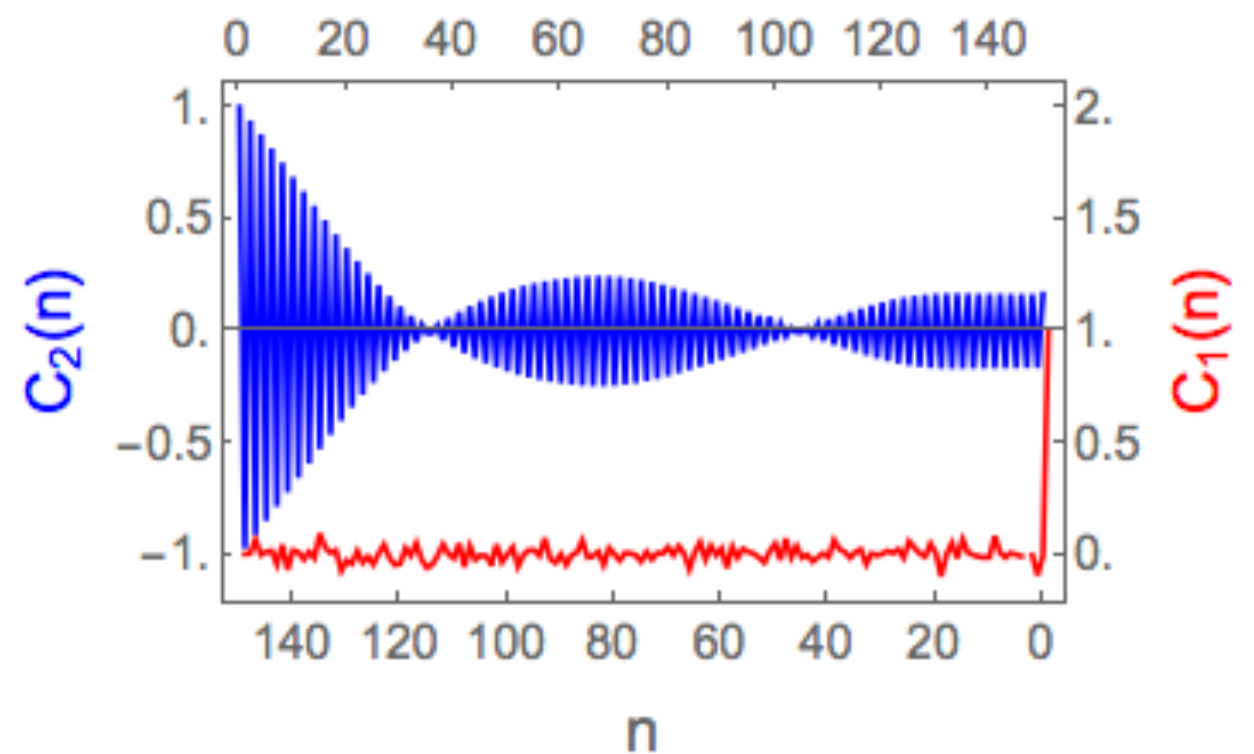
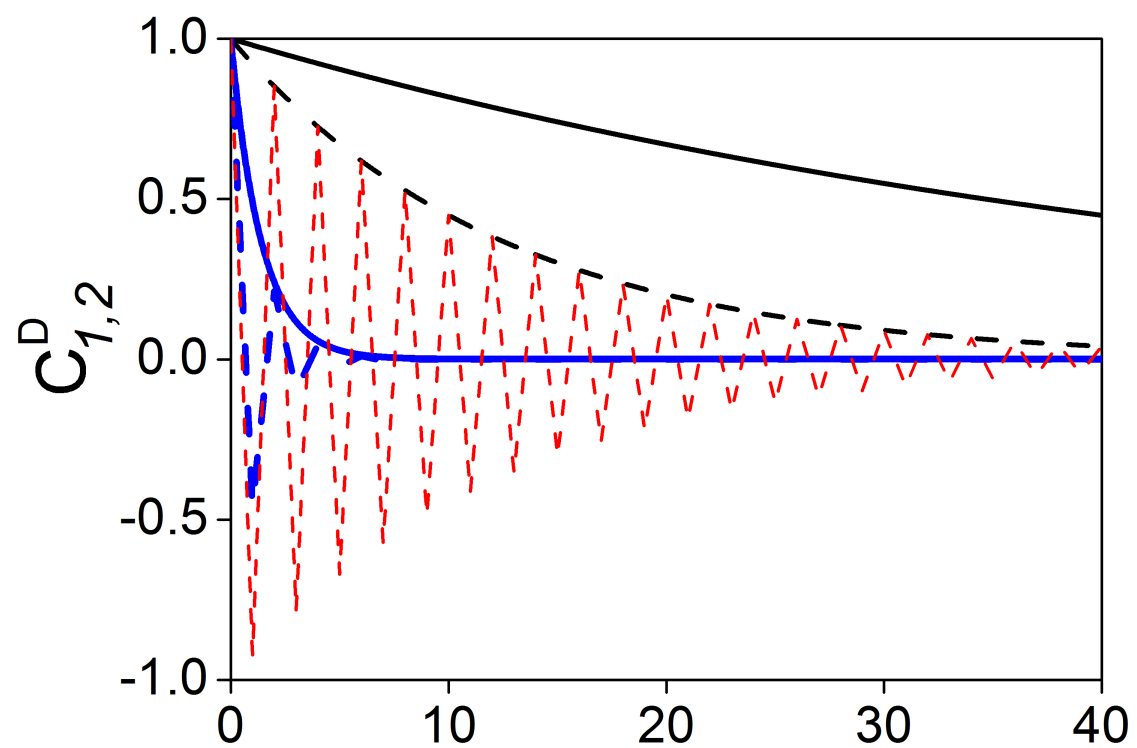
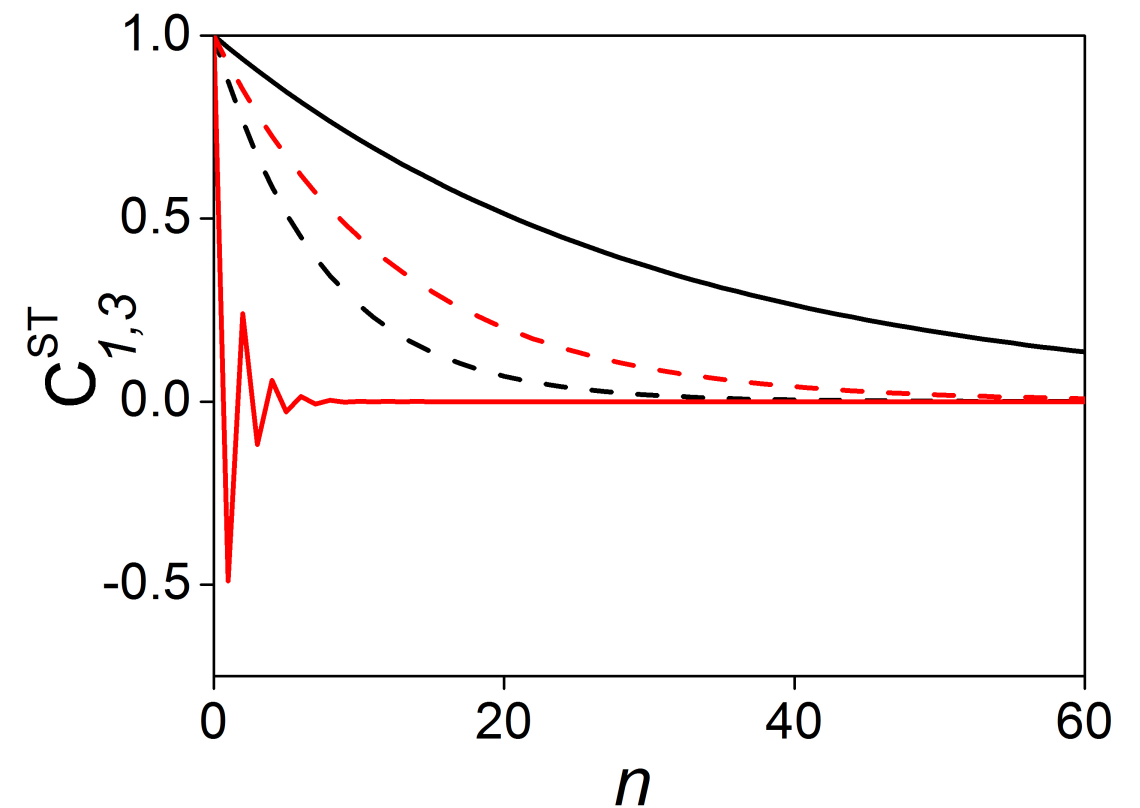
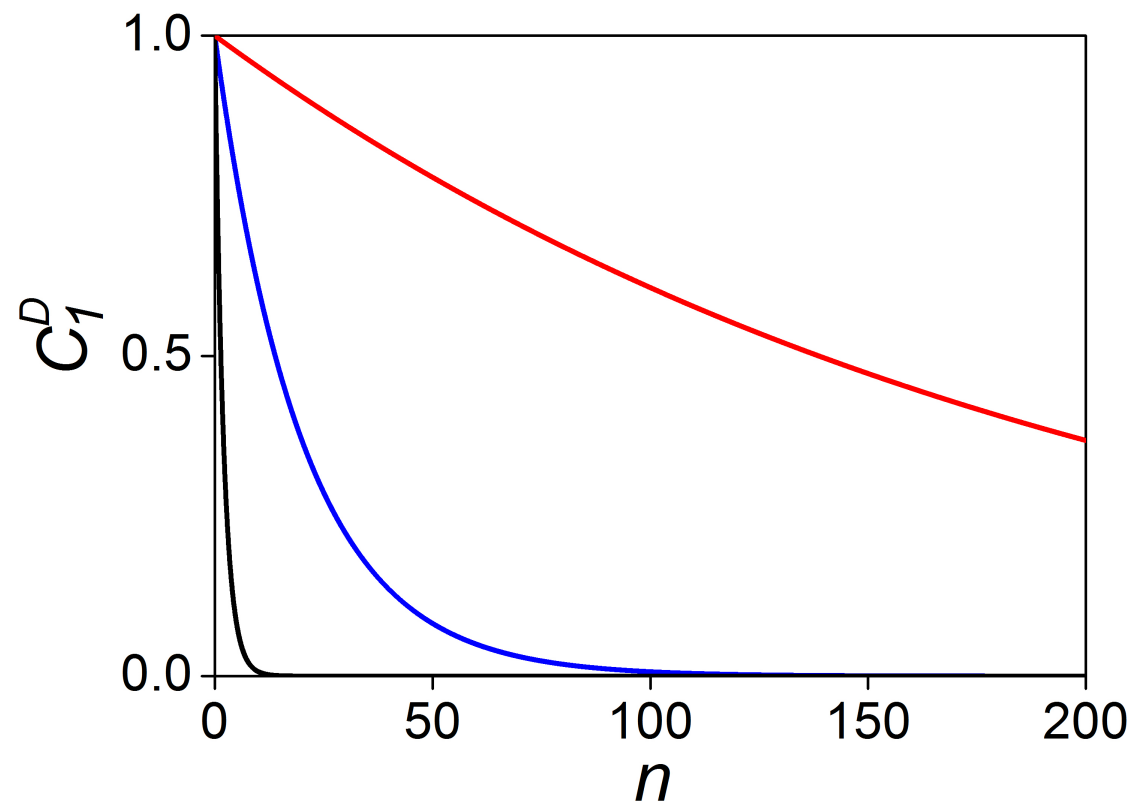
$$U\{\varphi_n\} = -E_J \sum_n \cos[\varphi_{+,n} - \varphi_{0,n}] + \cos[\varphi_{+,n} - \varphi_{0,n+1}] \\ + \cos[\varphi_{-,n} - \varphi_{0,n+1}] + (1 - 2f) \cos[\varphi_{-,n} - \varphi_{0,n}] \quad (12)$$

$$C_p^D(n) = \left\{ \frac{F_p^D}{F_0^D} \right\}^n \quad \alpha = 1 - 2f,$$

$$F_p^D = \int_0^{2\pi} du e^{ipu} I_0 \left[ 2K \cos \frac{u}{2} \right] I_0 \left[ K \sqrt{1 + \alpha^2 + 2\alpha \cos u} \right], \quad (13)$$

where  $K = E_J/(k_B T)$  and  $I_0(z)$  is the modified Bessel function.<sup>32</sup> For high temperatures  $k_B T \gg E_J$  ( $K \ll 1$ )

# DEGENERATE GROUNDSTATE AND CORRELATIONS



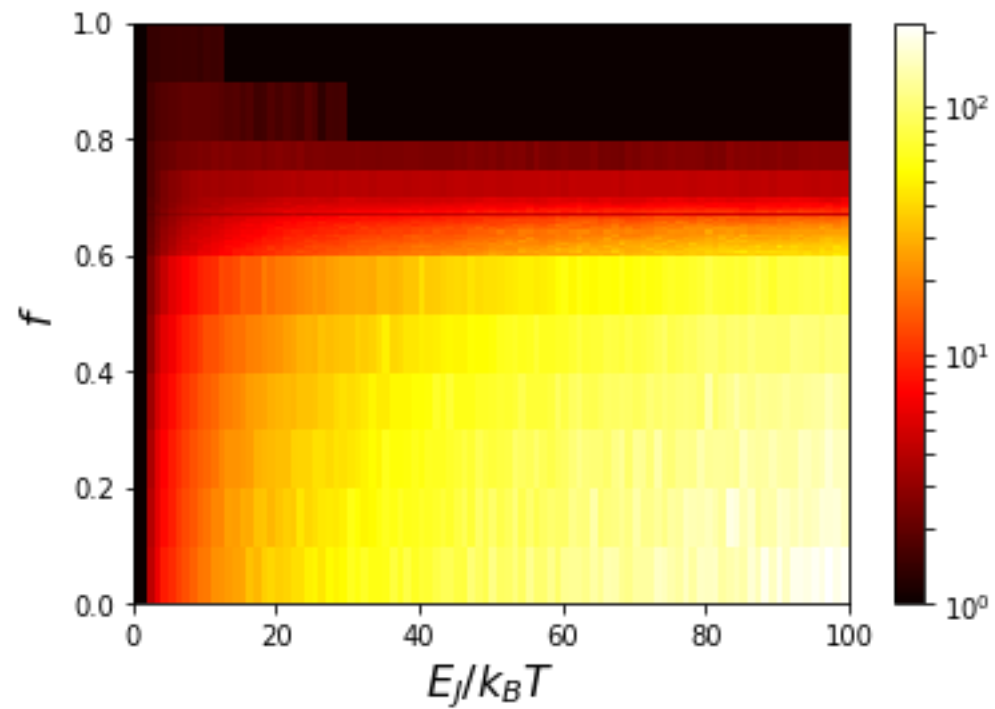


# CORRELATION LENGTHS

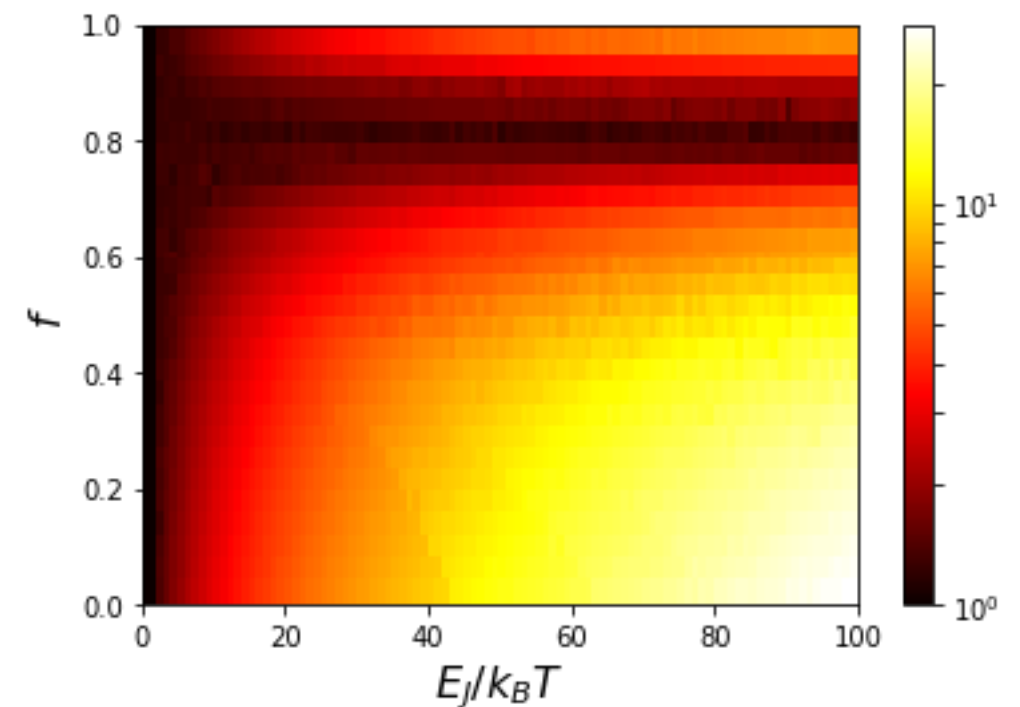
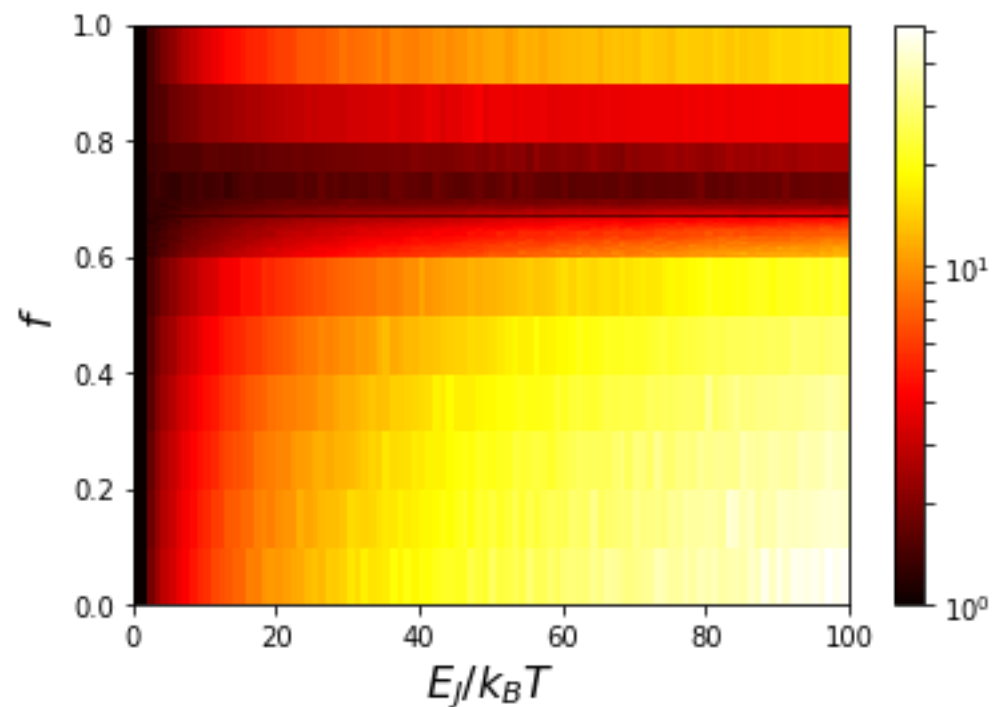
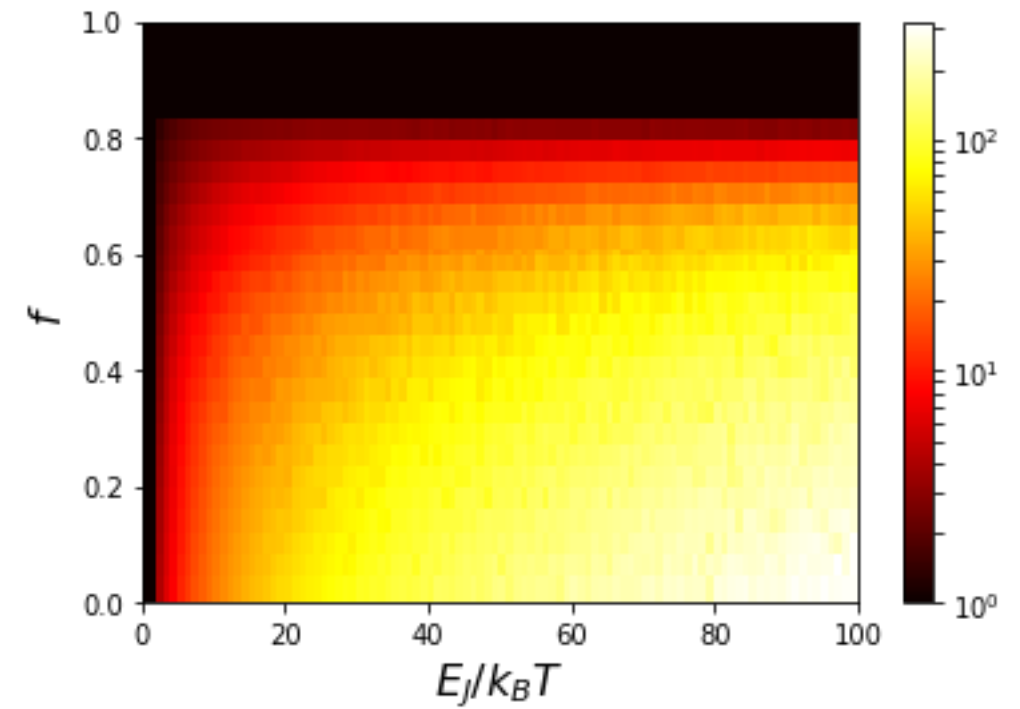
$$\xi_p = -\frac{1}{n} \ln C_p(n)$$

27

Diamond chain



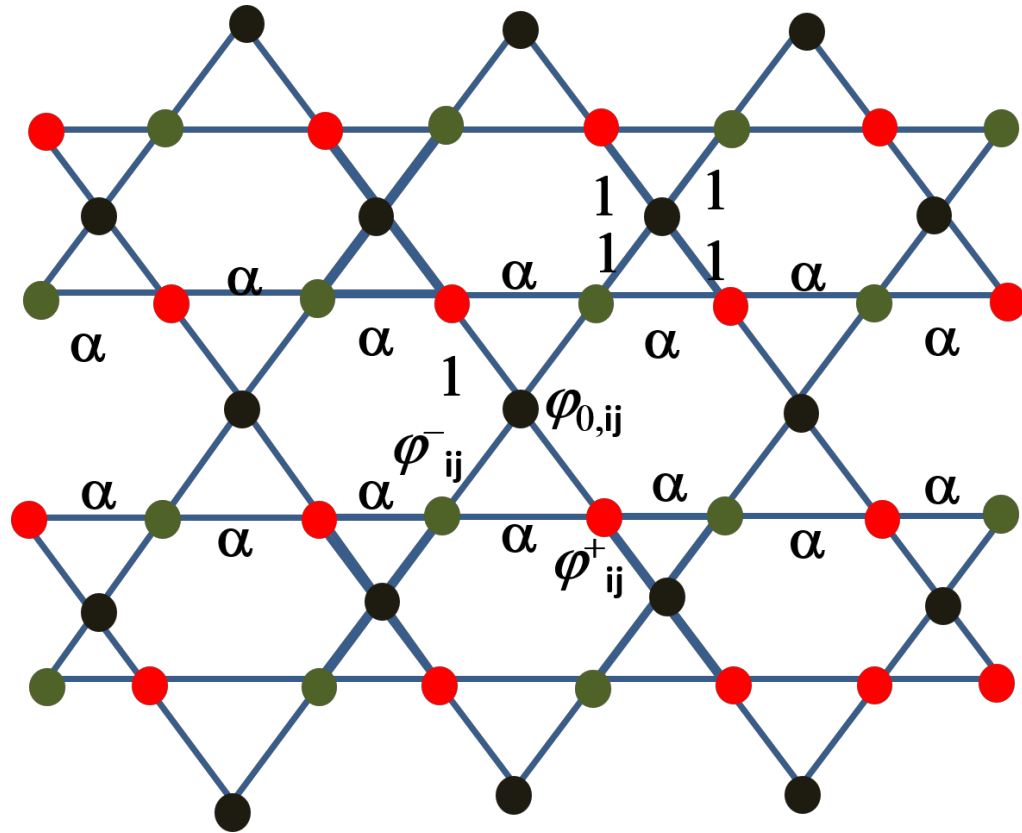
Sawtooth chain



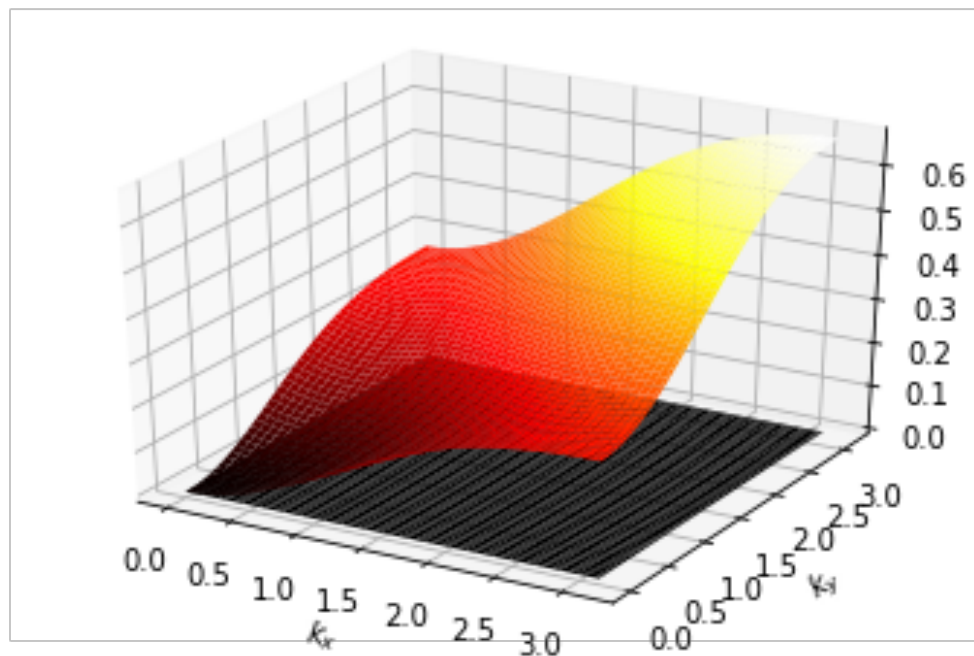
# **PART 3 – JOSEPHSON JUNCTIONS MEET MAGNETIC FRAGMENTATION**

# THE KAGOME LATTICE

29



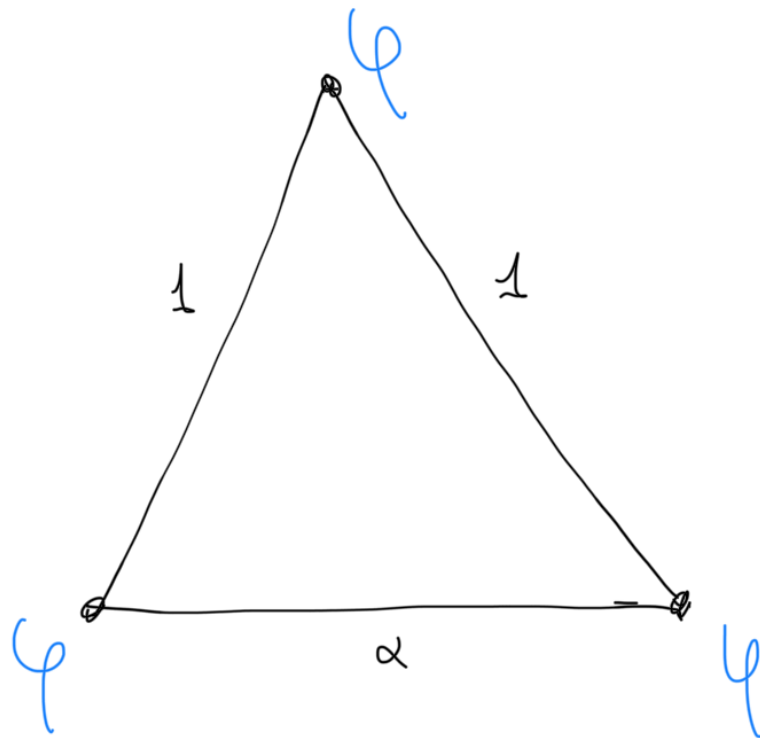
$$\mathcal{H} = - \sum_{\langle ij \rangle} J_{ij} \mathbf{s}_i \cdot \mathbf{s}_j$$



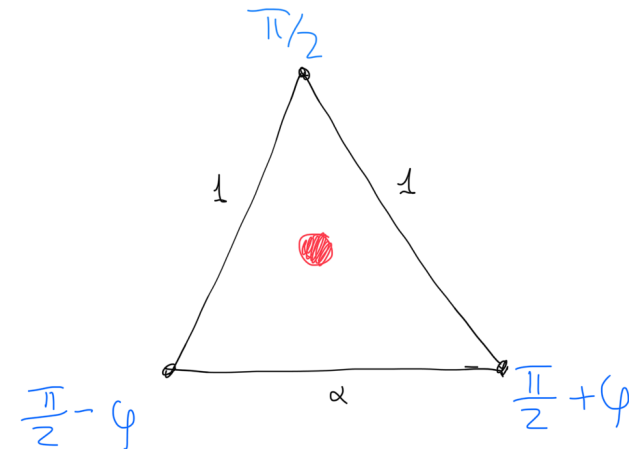
$$\begin{aligned} & \left[ -\frac{\omega^2}{\omega_p^2} + 4 \right] \left[ \left( -\frac{\omega^2}{\omega_p^2} + 2\alpha + 2 \right)^2 - 4\alpha^2 \cos^2 \frac{k_x + k_y}{2} \right] \\ &= 4 \left( \cos^2 \frac{k_x}{2} + \cos^2 \frac{k_y}{2} \right) \left( -\frac{\omega^2}{\omega_p^2} + 2\alpha + 2 \right) + \\ & \quad + 16\alpha \cos \frac{k_x + k_y}{2} \cos \frac{k_x}{2} \cos \frac{k_y}{2}. \end{aligned} \quad (9)$$

# SINGLE TRIANGLE GROUND STATES

$$\alpha > \alpha_c$$

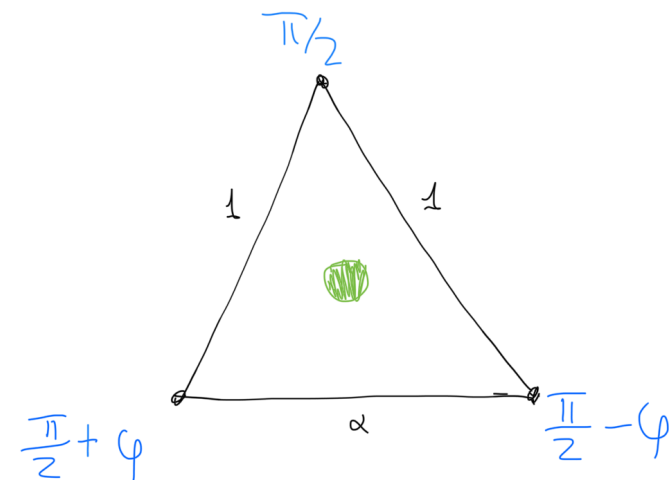


$$\alpha < \alpha_c$$



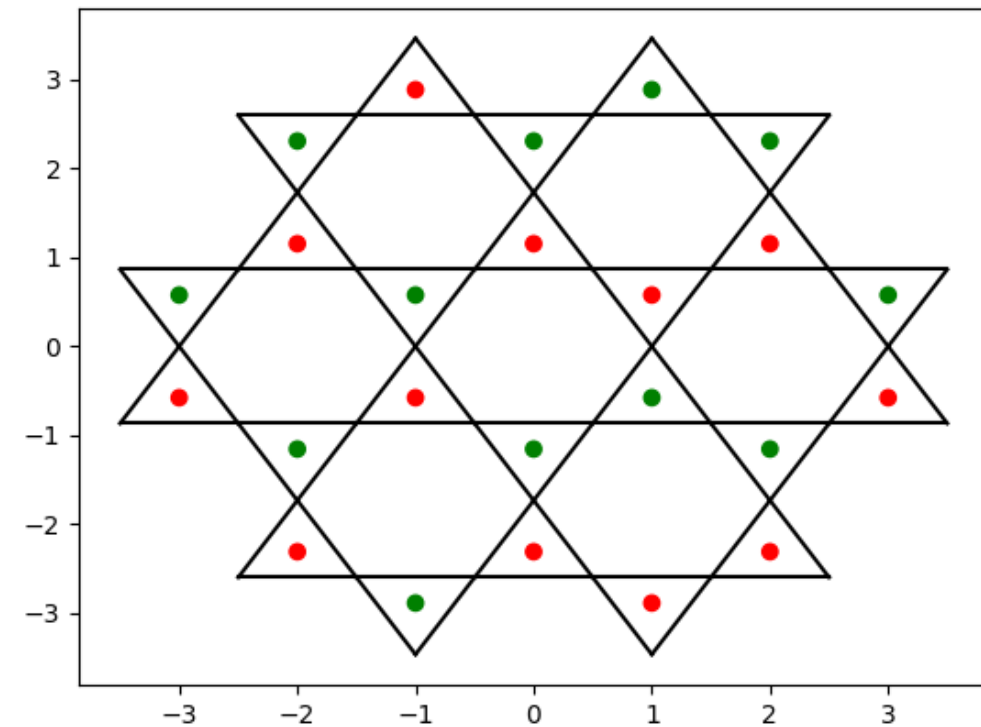
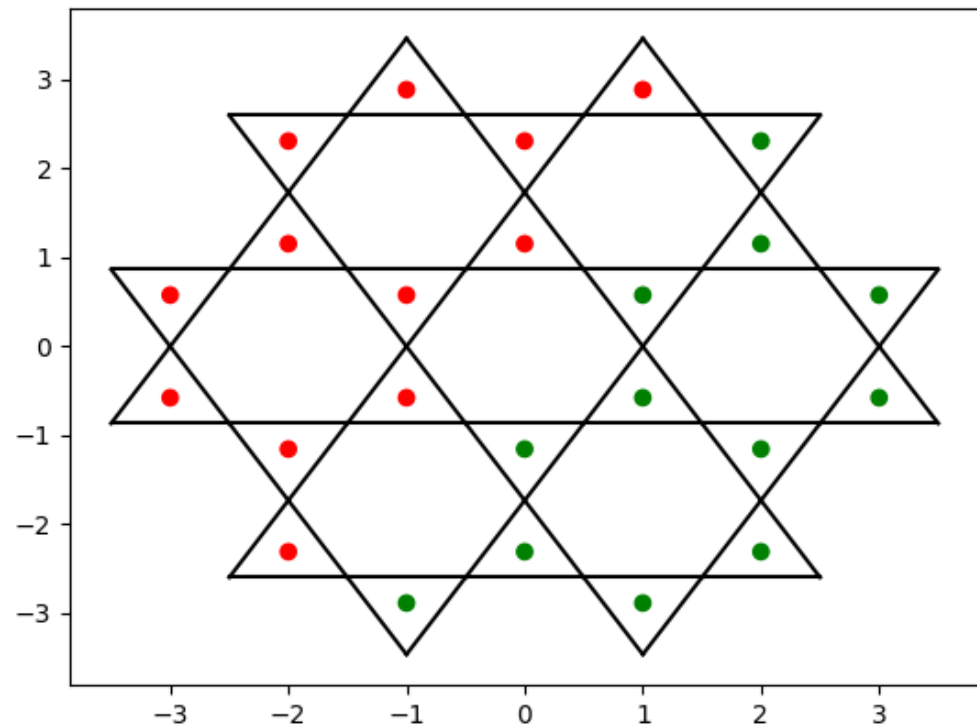
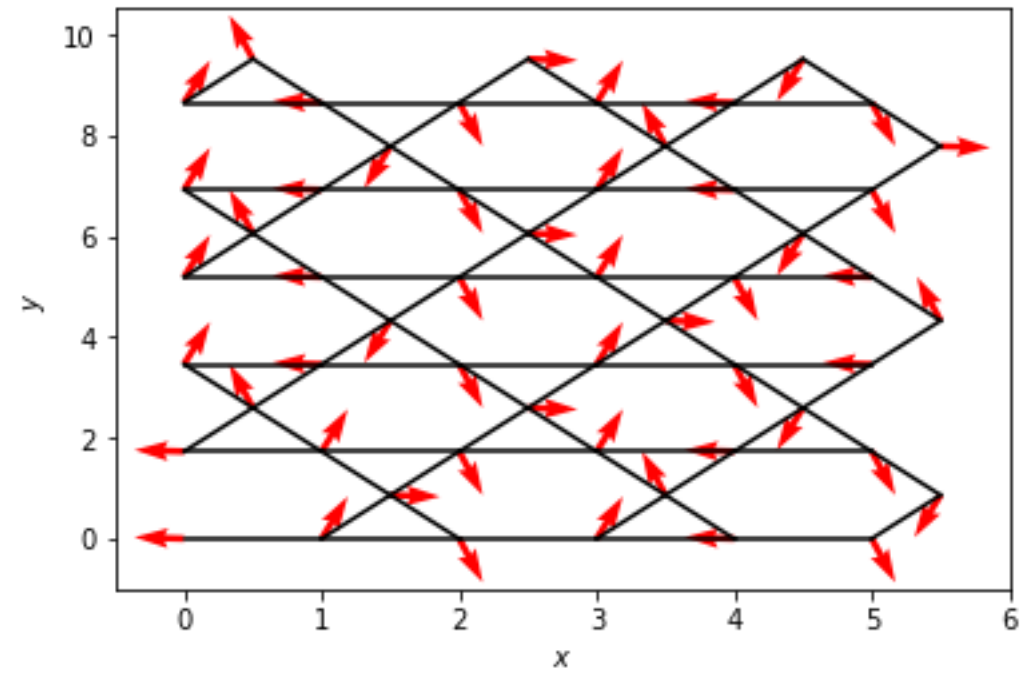
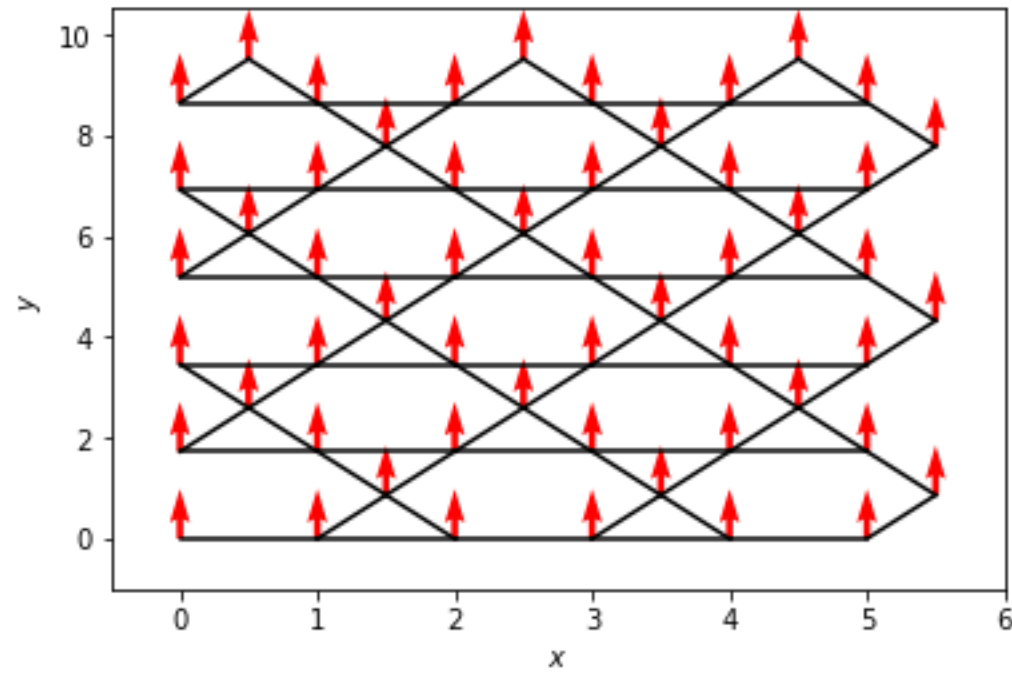
$$\varphi = \arccos\left(-\frac{1}{2\alpha}\right)$$

$$\alpha < \alpha_c$$

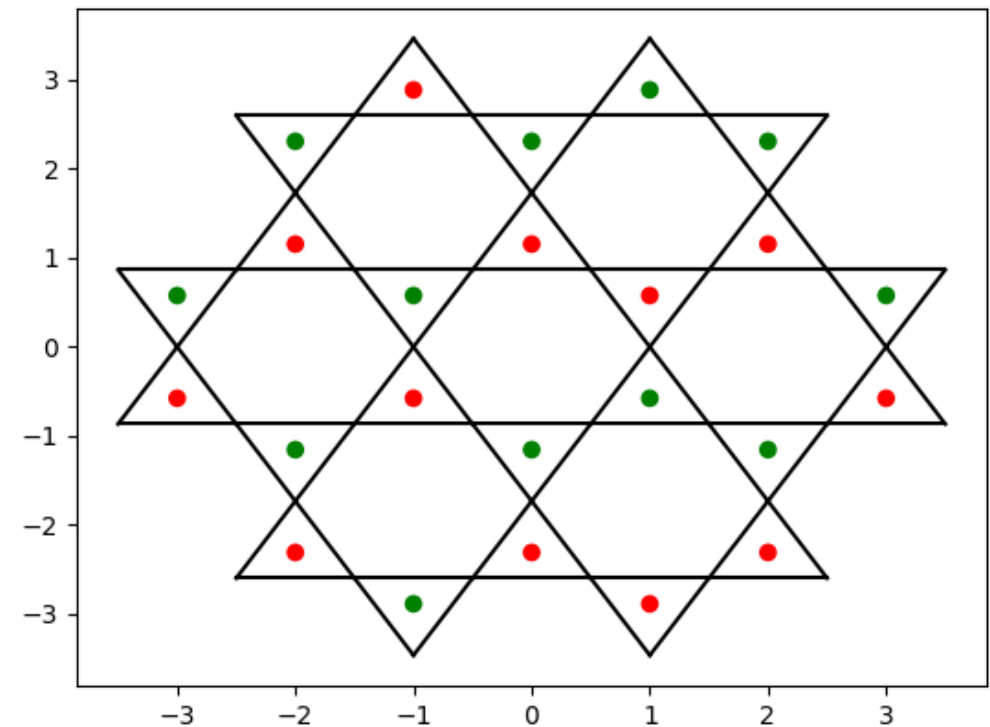
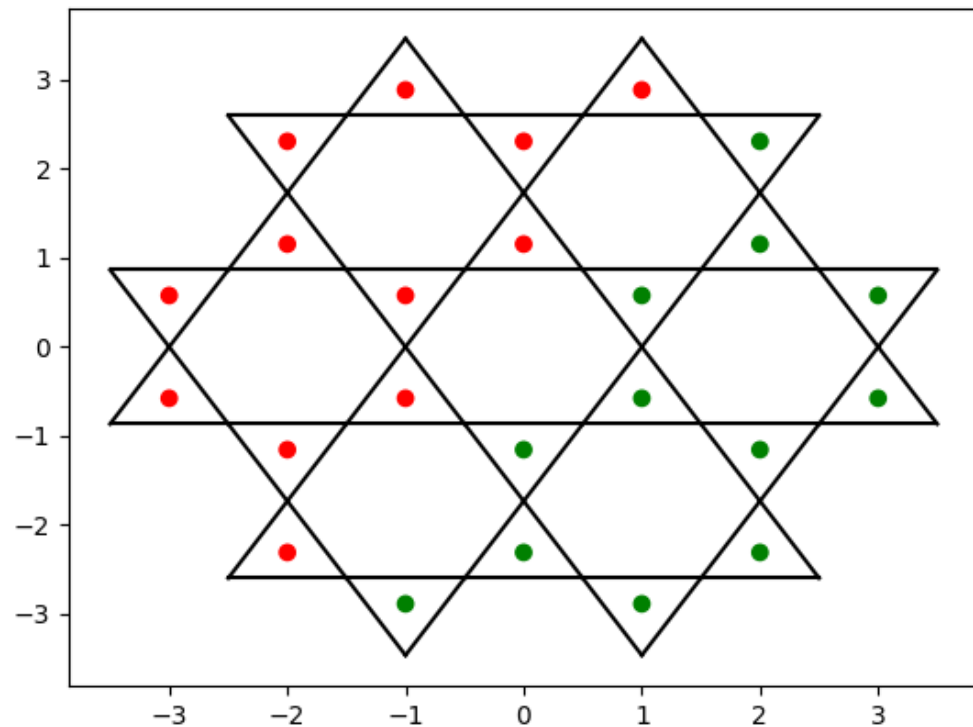


$$\varphi = \arccos\left(-\frac{1}{2\alpha}\right)$$

# THE GROUND STATES



# THE GROUND STATES: DESCRIPTION

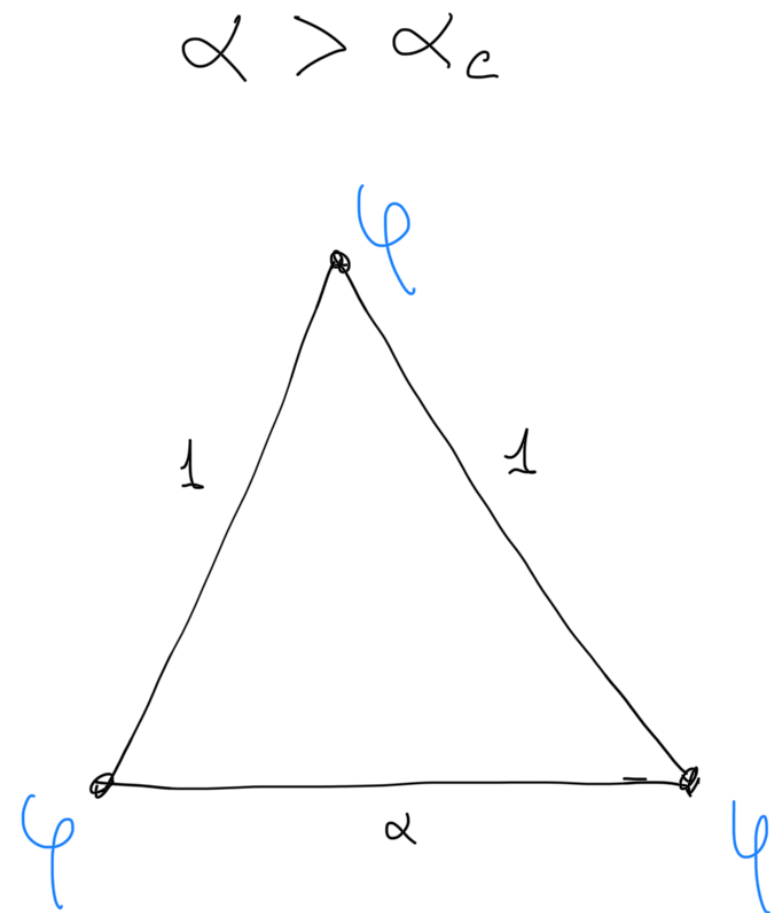
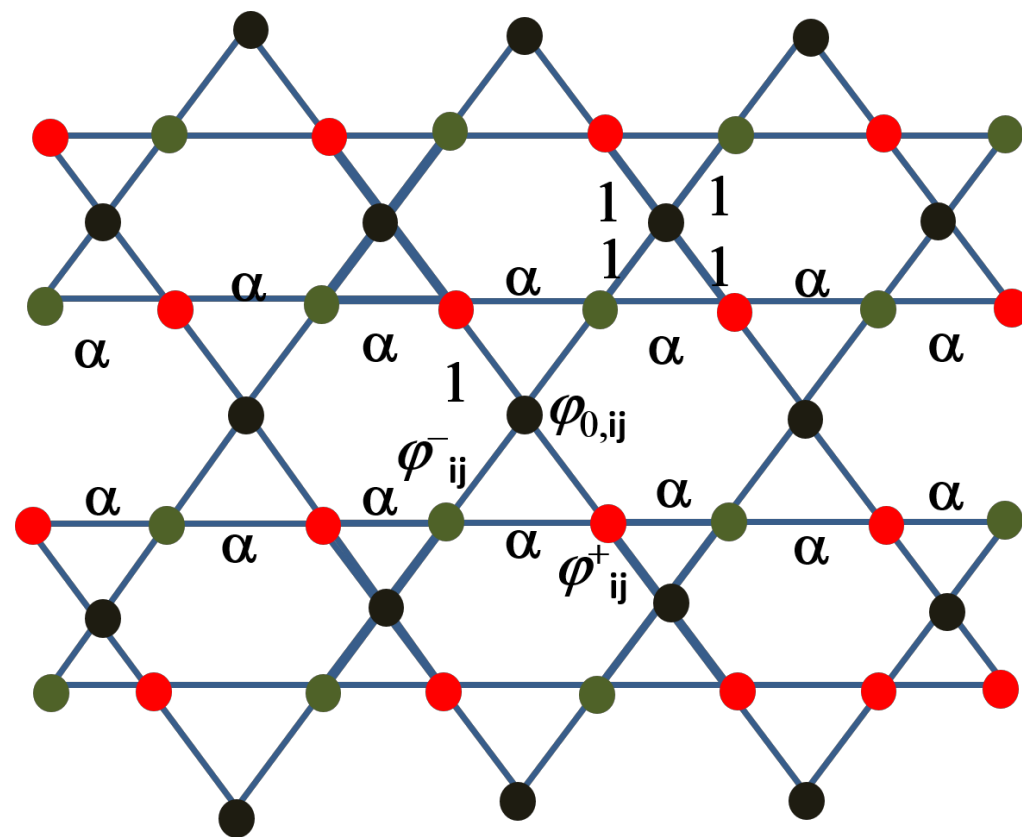


- ▶ Triangles in hexagons either have the same color, or equal number of colors, if top and bottom triangles have different colors
- ▶  $|\mathbf{S}_\Delta| = \text{const}$
- ▶  $\alpha = -1$  maps onto the kagome AFM

# THE GROUND STATES: DESCRIPTION

$\alpha = -1$  maps onto kagome AFM

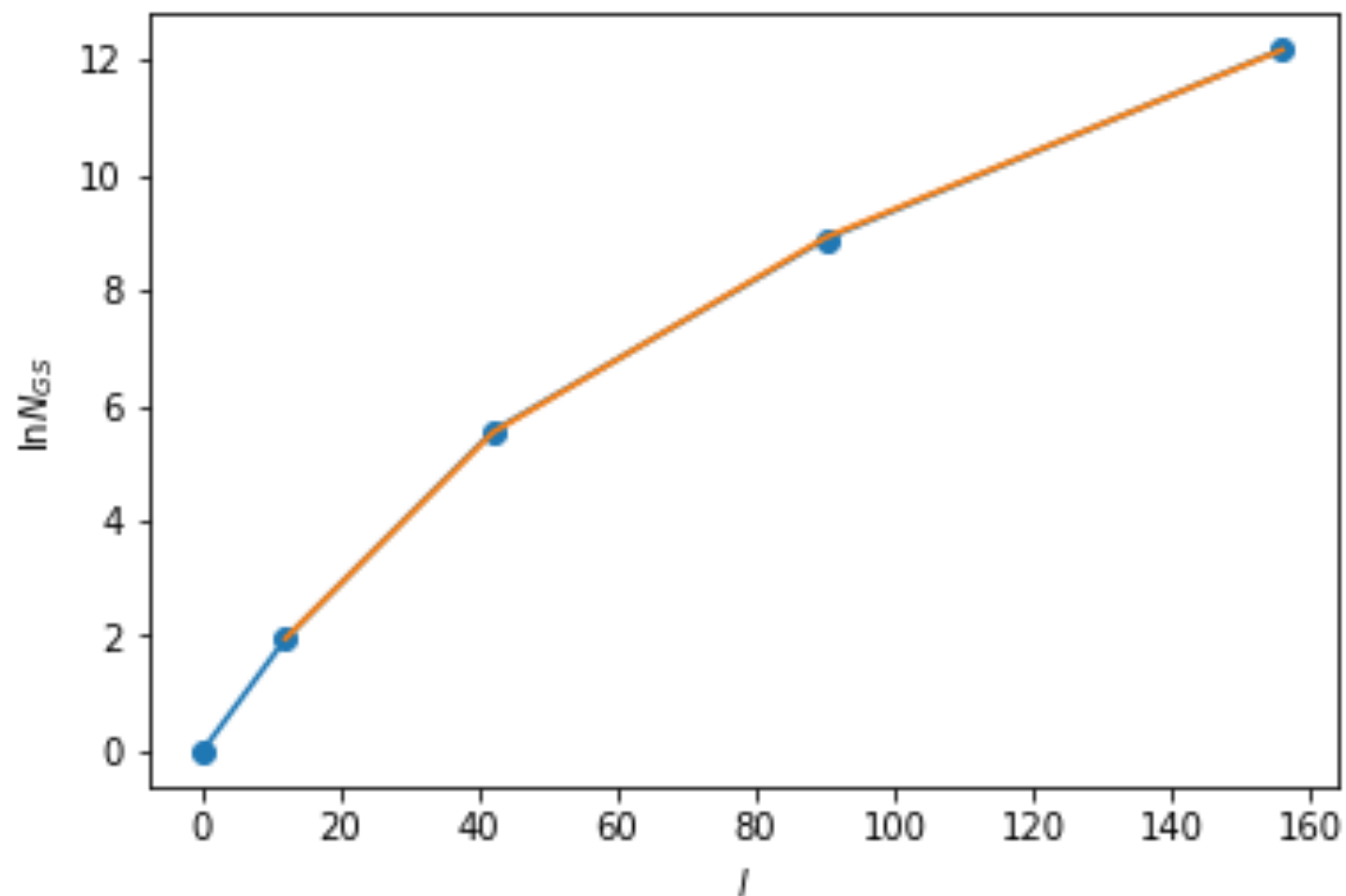
Groundstates = tricoloring the kagome lattice



# COUNTING THE GROUND STATES

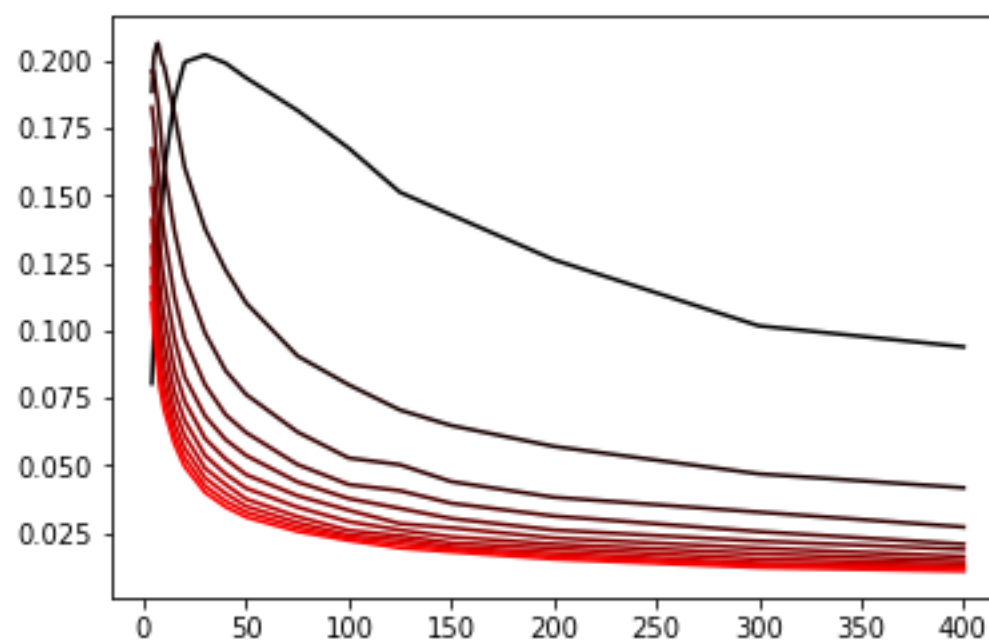
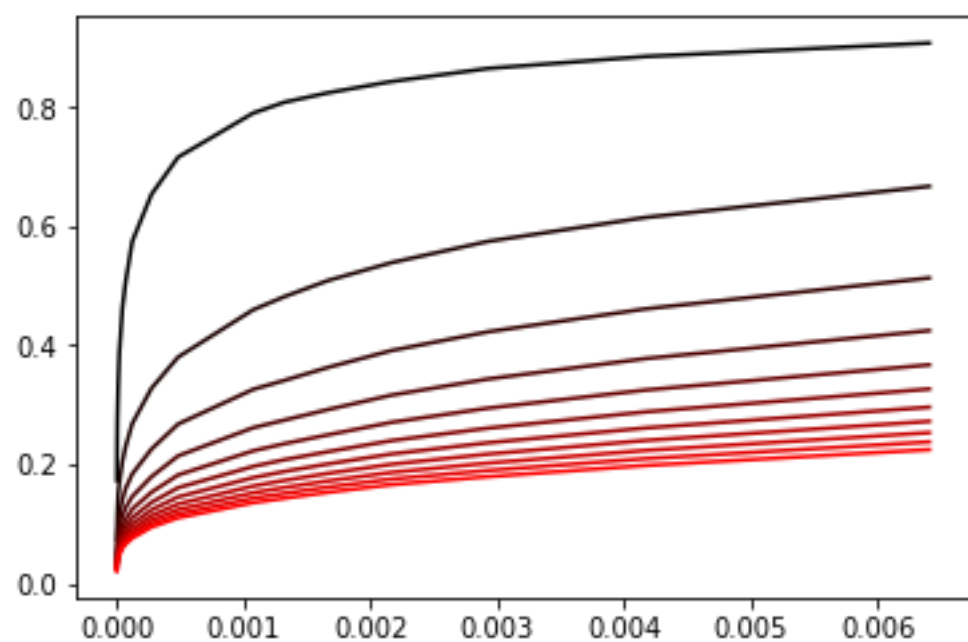
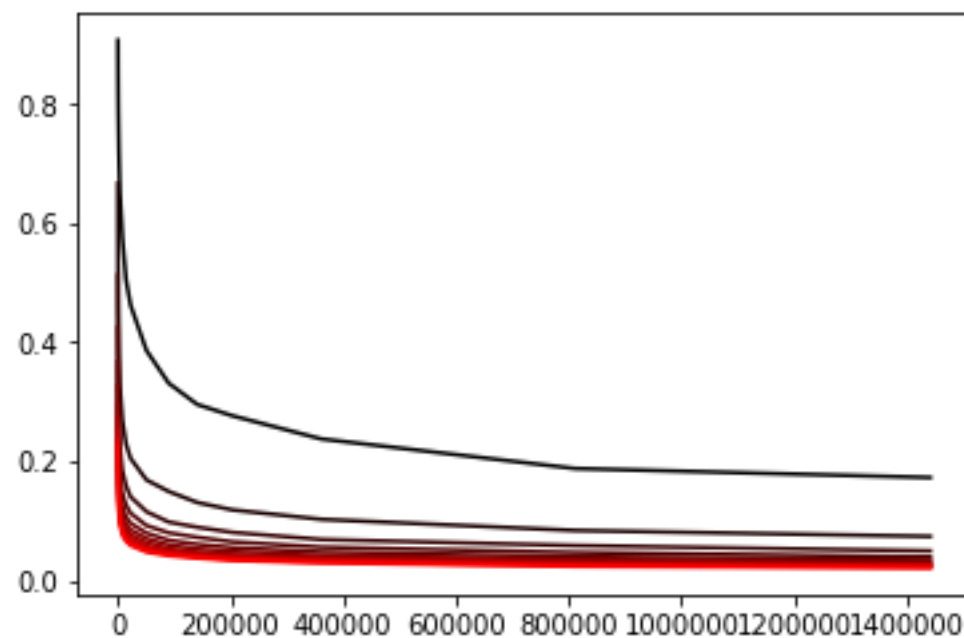
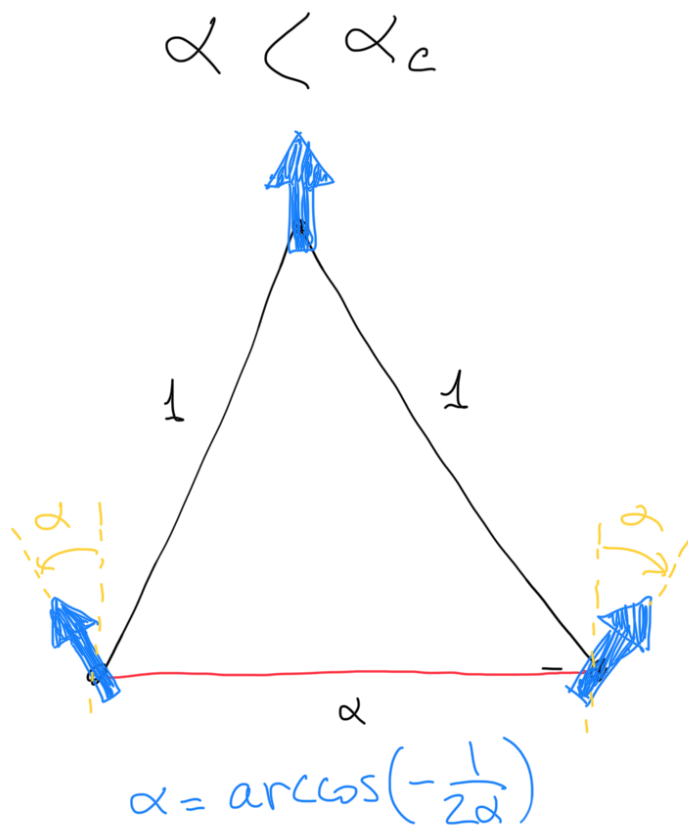
$$\alpha \neq -1 : \quad \ln N_{GS} \propto 0.23 \ln 2 N^{0.444}$$

$$\alpha = -1 : \quad \ln N_{GS} \propto 0.126 N$$

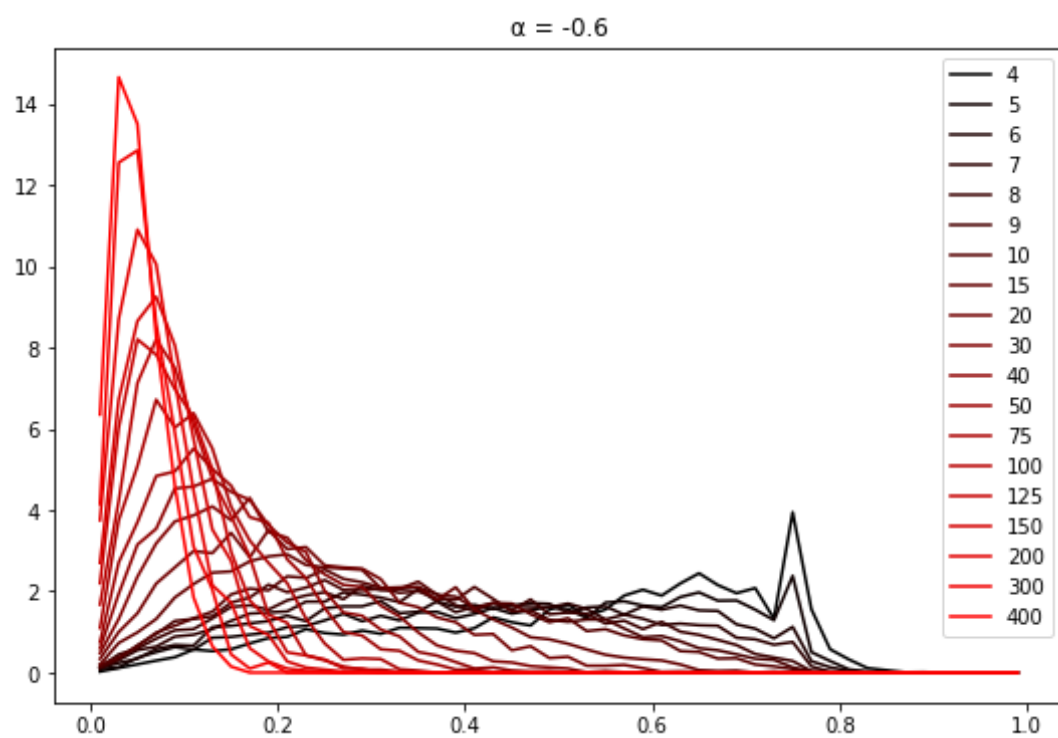
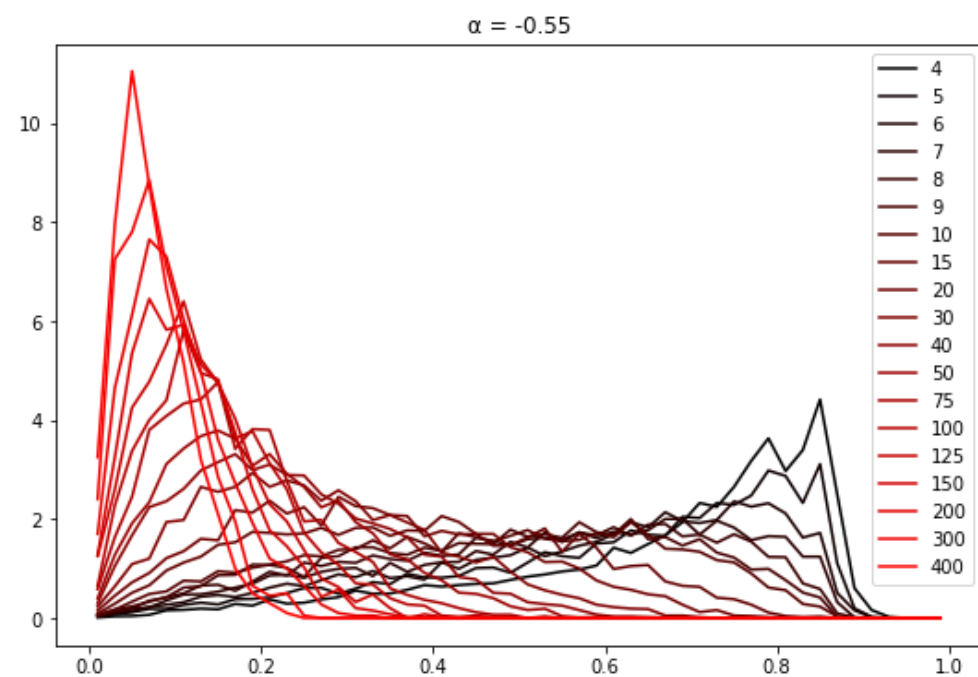
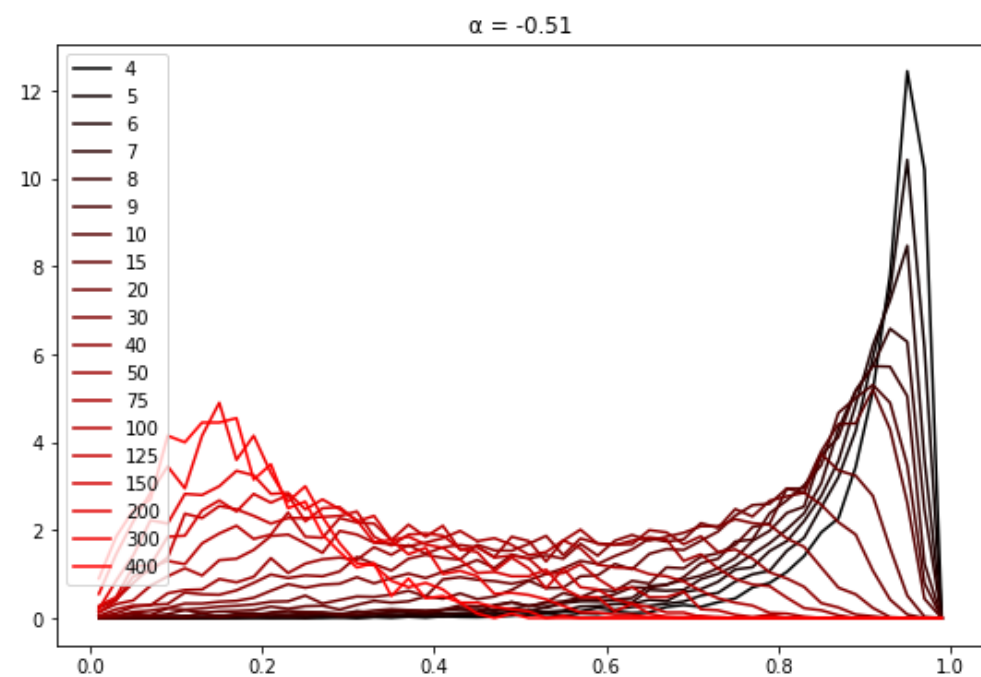




# THE GROUND STATES MAGNETIZATION



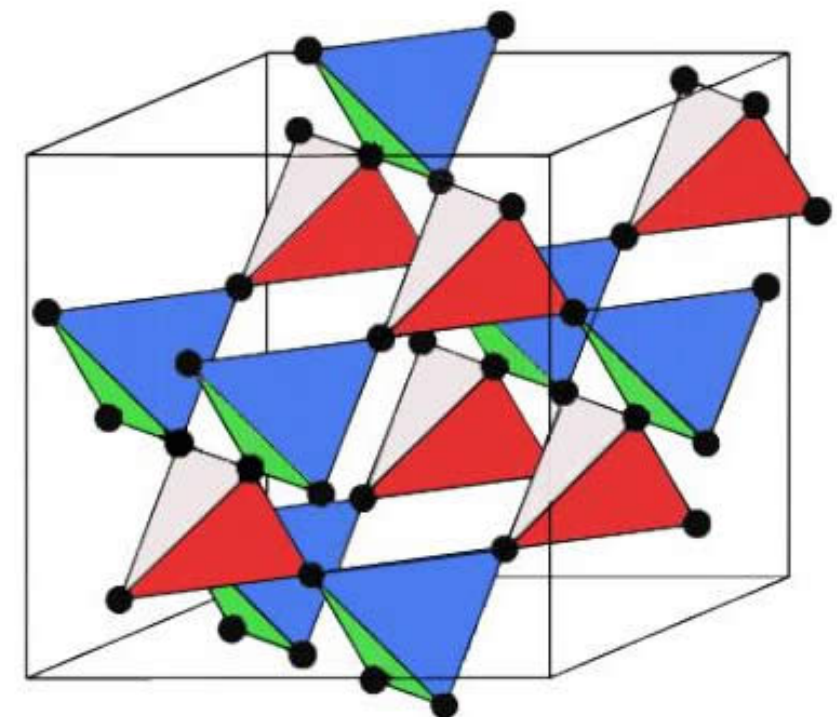
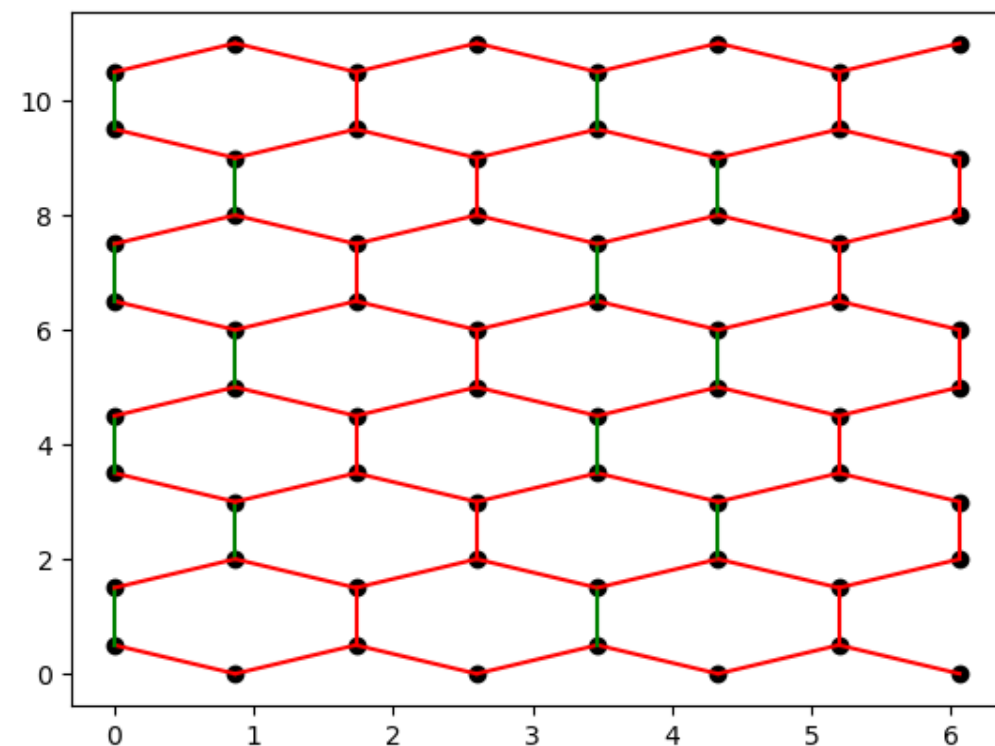
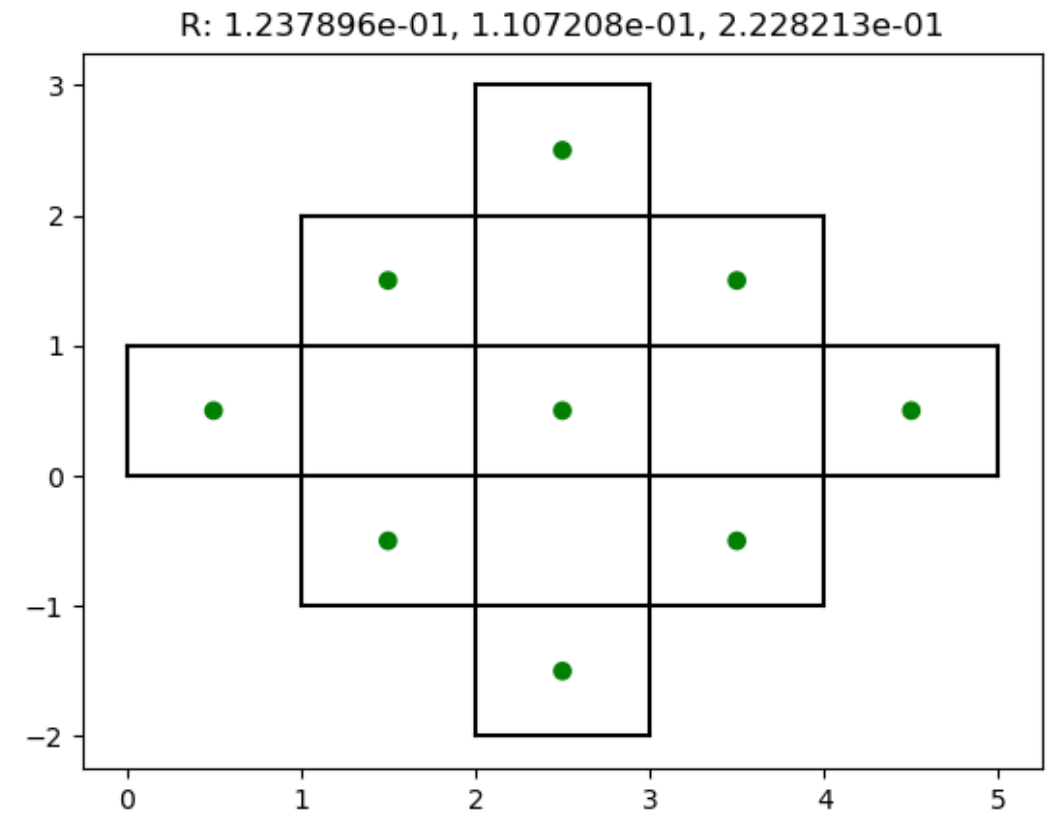
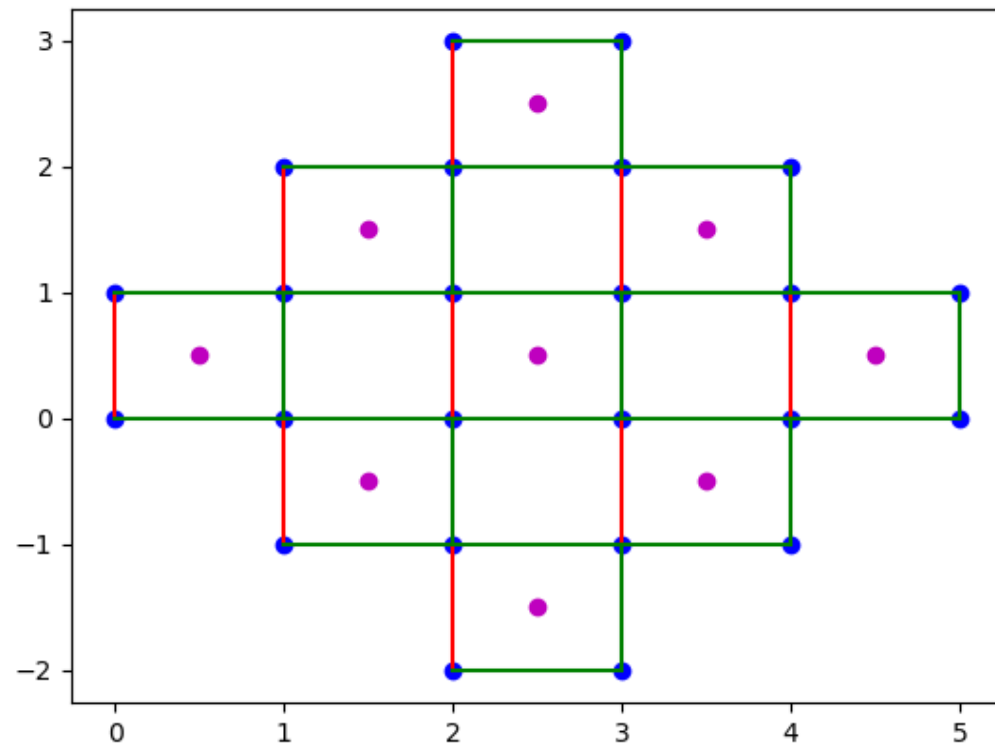
# THE MAGNETIZATION PDF



## TAKE AWAY MESSAGE

- ▶ classical XY model on the kagome lattice with explicit sublattice symmetry breaking
- ▶ Transition from uniform/ferromagnetic groundstate to frustrated, highly degenerate
- ▶ Degeneracy of the groundstates persists for a range of frustrations
- ▶ Restoration of order for specific frustrations in higher order correlation functions
- ▶ What happens if quantum fluctuations are added?
- ▶ Possible new highly degenerate Hamiltonians, also for Heisenberg spins

# OTHER LATTICES?





THANK YOU FOR YOU  
ATTENTION